N69-19029

NASA CR-100026

GCA-TR-68-12-N

ROCKET RELEASE OF TRIETHYL BORON

J. PRESSMAN

GCA CORPORATION
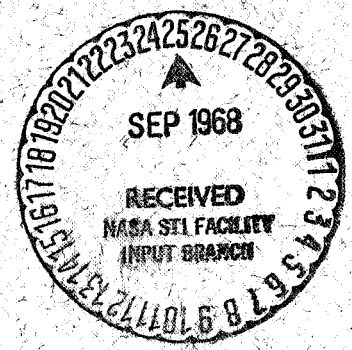
Bedford, Massachusetts

FINAL REPORT
CONTRACT NO. NASW-1419

ROCKET RELEASE OF TRIETHYL BORON

J. Pressman

GCA CORPORATION
GCA TECHNOLOGY DIVISION
Bedford, Massachusetts

FINAL REPORT

Contract No. NASW-1419

September 1968

Prepared for

NATIONAL AERONAUTICS AND SPACE ADMINISTRATION
Headquarters
Washington, D. C.

TABLE OF CONTENTS

ROCKET RELEASE OF TRIETHYL BORON

By Jerome Pressman
GCA Corporation

SUMMARY

This report describes an experiment in which two rockets, each carrying a compound payload consisting of a canister of triethyl boron (TEB) and a 5577Å photometer were used to probe the atomic oxygen region. One was fired at twilight February 21, 1968 and one during the night of February 26, 1968.

The nighttime flight reported a profile of the 5577Å emission which had a sharper lower boundary, a more rapid decrease with height and thus a much smaller half-width than previous similar altitude profile measurements. The differences are so great that the new measurements require verification even though they more closely resemble the theoretically expected profile. No TEB chemiluminescence was observed. This is due either to a malfunction of the release mechanism or actual lack of chemiluminescence in contradiction with laboratory data.

The twilight trail gave a fluorescence at least as bright as that of TMA. A new BO_2 band, not observed in previous twilight spectrum was recorded. The band is at 4072.2Å and assigned to the $X\ ^2\Pi_{o\frac{1}{2}}$ - $B\ ^2\Sigma^+$, 000 - 000 transition unlike the other transitions assigned to the X - A states.

I. INTRODUCTION

This report describes an experiment in which two rockets carrying a compound payload consisting of a canister of Triethyl Boron (TEB) and a 5577Å photometer were used to probe the atomic oxygen region. One was fired at twilight on February 21, 1968 and one during the night of February 26, 1968. In an earlier phase a rocket was fired on the night of March 30, 1967 but a telemetry failure prevented a successful flight. In the February 21, 1968 flight, the TEB twilight release was successful but the photometer malfunctioned. In the subsequent night launching the photometer was successful, but there was no indication of TEB chemiluminescence.

Preliminary analysis of the data indicates that the photometer design was sufficiently unique so that a very sharp lower edge of the 5577Å (oxygen green line) emitting region was measured in accord with theory. The TEB twilight trail appeared at least as bright as that of TMA and successful wind measurements were made. In the spectra a new band of the $X\ ^2\Pi_{0\frac{1}{2}}$ - $B\ ^2\Sigma^+$, $0\overset{0}{0}0$ - $0\overset{0}{0}0$ transition of BO_2 was observed for the first time in a release spectrum.

The general nature of the program and the conceptual design and the experimental plan is contained in Section II while Section III includes the original experimental design (prior to the March 30, 1967 firing). In Section IV is given a summary of the post-firing diagnosis of that launch while in Section V is given a description of the payload redesign and fabrication for the two subsequent flights. Finally in Section VI is furnished details of the rocket firing data and conclusions thereto of the February 1968 launches. These conclusions are based on a preliminary analysis. The night-time release of TEB is for the purpose of obtaining improved data of winds, turbulence-like structure, and relative concentration of atomic oxygen. Such data are of inherent value in extending our knowledge of space and time variation of such variables. The number of such measurements is as yet quite limited. TEB was selected on the basis of laboratory measurements (see below) as having weight advantage over TMA.

II. OUTLINE OF PROGRAM

A. Conceptual Design

1. **Purpose.** — This experiment involved the firing of two Nike Apache rockets, one at night and one at twilight. Each rocket contained a combined payload consisting of a canister of triethyl boron (TEB) and a narrow-band special-purpose photometer designed to look upward for measuring the atomic oxygen emission at 5577Å. Inclusion of the photometer permits (to some extent) a cross correlation of this airglow with the chemical release luminosity. In addition to four camera sites, the ground equipment also included a 5577Å photometer as well as a Fastie spectrometer for measuring the chemical release spectra.

The two rocket experiments using the Nike Apache, one at night and one at twilight, represented a multiple measurement experiment possessing inner correlation because of the simultaneous measurement of several variables and proposing to elucidate some of the major properties of the state of the upper atmosphere from approximately 80 to 140 km. The nighttime experiment has for its aim the measurement of 5577Å on the way up and release of TEB in a trail on the way down. In this particular arrangement, the photometer can make measurements of the normal 5577Å emission unpolluted by the TEB chemiluminescence or fluorescence. Further, no risk was seen of the TEB coating or damaging the optical instruments.

The measurement of the vertical distribution of 5577Å is a basic one of intrinsic value in itself. Such measurements do not exist in satisfactory number and quality, so that the space and time variation of the vertical distribution of 5577Å in the upper atmosphere is not definitively demarcated at this time. Consequently, the mechanism of this emission is not well established.

The nighttime release of TEB was intended to provide improved data of winds, turbulence-like structure and relative concentration of atomic oxygen. Such data are of intrinsic value in further extending our knowledge of the space and time variation of these variables since the number of such measurements is as yet quite limited. TEB was selected on the basis of laboratory measurements (see below) as having weight advantages over TMA.

Further, a cross correlation was proposed to be made of the vertical variation of the intensity of the 5577Å emission and the TEB (or aternate) luminosity. Such a cross correlation would be advantageous to elucidating the mechanism of both emissions although primarily it is the organometallic emission which stands in greater need of clarification.

The twilight flight had an identical payload measuring 5577$\overset{\circ}{A}$ on the way up and releasing the TEB (or alternate) on the way down. The measurement of 5577$\overset{\circ}{A}$ during twilight is again of value. Since little twilight enhancement is expected theoretically the measurement should give us an indication of the variation of atomic oxygen during the night in the altitude from 80-120 km. The organometallic release had as its subsidiary purpose that of obtaining measurements (with a Fastie Spectrometer) of the band structure in order to ascertain its utility in making temperature measurements.

Additionally, measurement of wind, diffusion at upper levels and turbulence-like structure of the lower levels were proposed. The use of a different chemical compound with different thermochemical and reactive properties it was considered should enable a clearer determination of whether the "turbulence" observed is an atmospheric property or is due to chemical reaction with the contaminant. Again these are measurements of intrinsic value in terms of their fitting into and extending the current incomplete picture of the upper atmosphere. Photometric and spectrometric measurements in comparison with the nighttime measurements were to be made to determine the extent possible the chemiluminescent and fluorescent contribution to the twilight luminosity. If possible, the relative atomic oxygen concentration at twilight and at night were to be deduced from the observation.

It was intended that comparisons be made between the rocket twilight luminous TEB trail (or chemiluminescent portion thereof) and the rocket 5577$\overset{\circ}{A}$ emission at twilight so as to elucidate the respective mechanisms. The ground 5577$\overset{\circ}{A}$ photometer was also to serve as a calibration check on the rocket photometer and also on the down leg to determine the extent to which any 5577$\overset{\circ}{A}$ enhancement occur on the release of TEB.

2. <u>Technological Purposes.</u> — The use of TEB was considered to offer a possible alternative to Trimethyl Aluminum (TMA). The lighter payloads as indicated by laboratory experiments it was considered might find application in the NASA and international rocket programs of wind, diffusion, and turbulence measurements in the upper atmosphere. Improved chemical compounds should facilitate combined payloads because of weight saving and also because of longer duration trails should render measurements more precise.

3. <u>Spectroscopic Discussion.</u> — Trimethyl aluminum in the upper atmosphere has been used to study winds, diffusion, and upper atmospheric temperature. Initial data obtained in the laboratory indicated that the intensity of the glow produced during the gas phase reaction of atomic oxygen and triethyl boron is more chemiluminous than that of atomic oxygen and trimethyl aluminum. The same photometric and spectrographic system can be used for the study of luminous trails produced by the release of triethyl boron in the upper atmosphere. There are summarized here, the previous observations of the trimethyl aluminum trails.

The nighttime and twilight release of trimethyl aluminum was first reported by Rosenberg, et al (Ref. 1, 2). The nighttime release was initiated around 94 km. The trail was visible to naked eye and could be photographed up to 1000 seconds after the release. The trail could be photographed with a f/2.5 and 175-mm focal length camera on a Royal-X Pan film with an exposure time of 5 seconds. Approximately 8×10^{24} molecules of TMA were released, of which about 2×10^{24} were available in the vapor phase and rest were frozen. These numbers are quoted for TMA since similar (actually somewhat better) statistics are applicable to TEB.

Twilight release was observed between 95 km and 150 km with a release rate of 20 grams per 1-km altitude. The solar horizon at the time of release was at 110 km. The twilight spectrum of AℓO was recorded with a slitless grating spectrograph of aperture f/0.87 and 76-mm focal length, with a grating of 1800 line/mm. The exposure time required with a RXP film was 30 seconds.

For the experiment using TEB, the decision regarding the film and the spectrograph characteristics depends on the spectral distribution of the chemiluminous glow and on the band systems of BO expected to fluoresce during the twilight release. These are discussed below.

The spectrum of the chemiluminescence produced during the reaction of triethyl boron and atomic oxygen has been previously studied (Ref. 3) and is shown in Figure 1. For comparison, the spectral distribution of the chemiluminescence produced during the reaction of some other organometallic compounds has also been included in Figure 1.

The wavelength of the bands of the BO-band system which are expected in the spectrum of the illuminated twilight release of triethyl boron is collected in Table 1 (Ref. 4).

It can be seen from Figure 1 that the chemiluminous intensity peaks around 4400Å. From spectroscopic data, it is known that the 0 to 0 band of the alpha-system of BO (Table 1) is around 4250Å. Therefore, the photometric and spectrographic system should have the peak sensitivity around 4300Å. The light gathering power of both systems should be the same as that used in TMA release observations since both the chemiluminescent and fluorescent efficiencies of TEB are similar to those of TMA.

B.   Experimental Plan

This section outlines engineering and field operations. Details of the photometer design are furnished in Section III.A with the basic experimental designs stated in this section. Payload design details (electronic plus chemical payload) are furnished in Section III.B; field observation in Section VI.
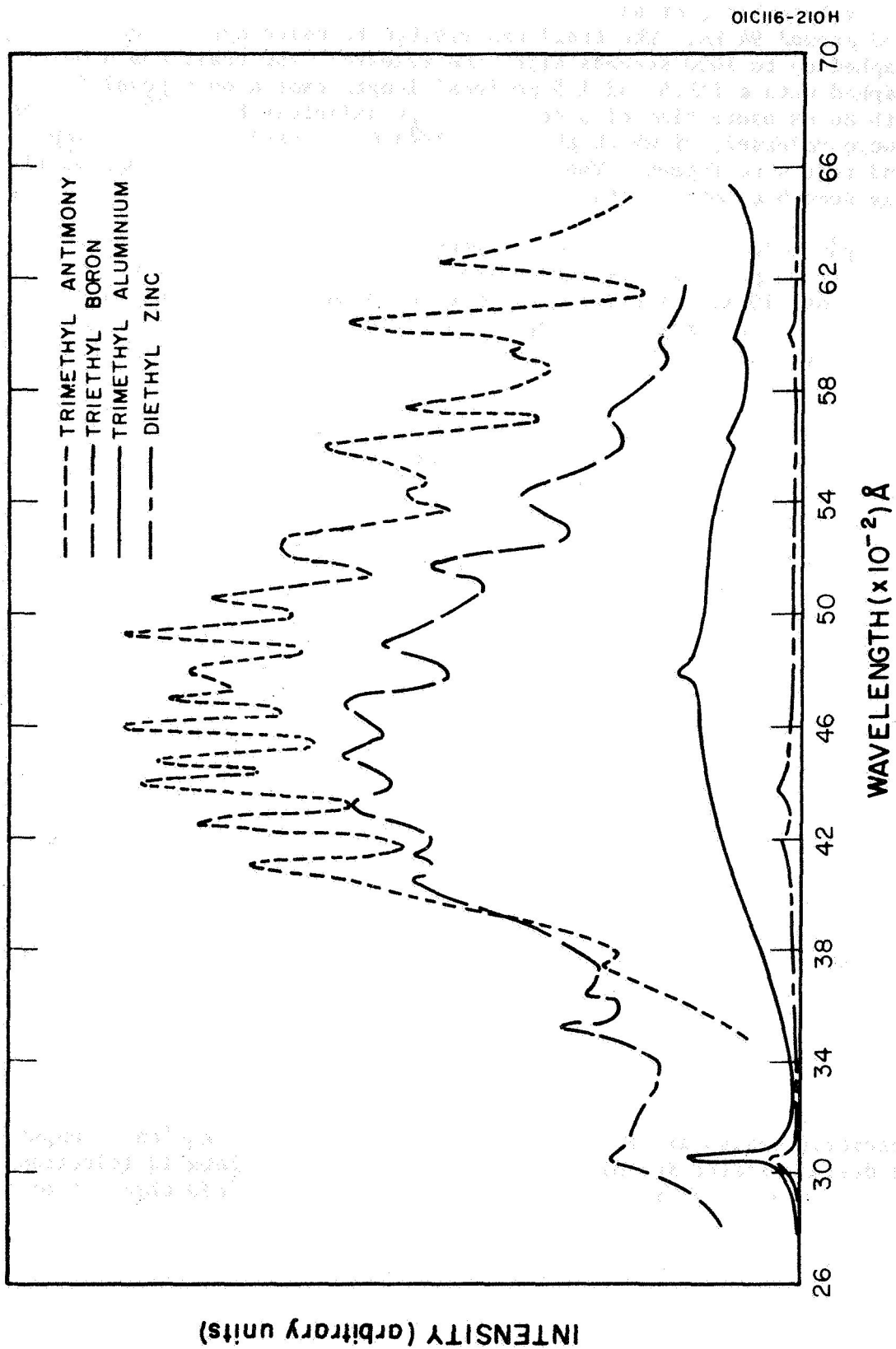
Figure 1.   The spectra of the chemiluminous reactions of some organometallic compounds
with atomic oxygen: the relative intensity of the different chemiluminous
reactions is shown.

TABLE 1

α-SYSTEM (A $^2\Pi$ - X $^2\Sigma$) OF BO (Ref. 4)

λ (Å)	I Visual Estimate	Transition (v',v'')	λ (Å)	I Visual Estimate	Transition (v',v'')
6165.4	5	$0,4\,O_1$	4247.9	4	$0,0\,R_1$
6159.7	5	$0,4\,R_1$	4227.5	4	$0,0\,R_2$
5551.5	8	$0,3\,O_1$	4145.5	7	$2,1\,O_1$
5547.5	7	$0,3\,R_1$	4143.4	6	$2,1\,R_1$
5513.0	5	$0,3\,R_2$	4124.1	4	$2,1\,R_2$
5043.5	6	$0,2\,O_1$	4037.4	8	$1,0\,O_1$
5040.1	9	$0,2\,R_1$	4035.5	7	$1,0\,R_1$
5011.6	4	$0,2\,R_2$	4017.1	6	$1,0\,R_2$
4746.9	8	$1,2\,O_1$	4015.0	5	$1,0\,R_{21}$
4744.0	8	$1,2\,R_1$	3950.5	4	$3,1\,O_1$
4718.7	5	$1,2\,R_2$	3848.7	10	$2,0\,O_1$
4715.5	5	$1,2\,R_{21}$	3847.0	9	$2,0\,R_1$
4615.4	10	$0,1\,O_1$	3829.9	8	$2,0\,R_2$
4612.7	10	$0,1\,R_1$	3828.0	6	$2,0\,R_{21}$
4588.8	8	$0,1\,R_2$	3679.1	10	$3,0\,O_1$
4585.7	7	$0,1\,R_{21}$	3677.8	8	$3,0\,R_1$
4365.9	8	$1,1\,O_1$	3662.3	6	$3,0\,R_2$
4363.4	10	$1,1\,R_1$	3660.6	5	$3,0\,R_{21}$
4341.9	8	$1,1\,R_2$			
4339.4	8	$1,1\,R_{21}$			
4250.4	5	$0,0\,O_1$			

1. Engineering and Field Phase. — Two rocket payloads were prepared and assembled for firing. The payloads consist of dispensers for releasing TEB (similar to those used for TMA) and narrow band photometers for measuring the 5577Å emission. Aspect is determined by a magnetometer and the magnitude of the 5577Å signal. Adequate timers and release indicators are used to insure release. Appropriate telemetry is installed. A 5577Å ground photometer, cameras, and Fastie-Ebert spectrometer were scheduled for field use. The ground photometer was operated by Dr. E. Manring of North Carolina State Teacher's College. The spectrometer was operated by Mr. J. Meriwether, Jr., under the direction of Mr. Fastie, University of Maryland.

In the field phase, two Nike Apache rockets with TEB and photometer payloads were to be fired; one under nighttime conditions and the other during appropriate twilight conditions.

The proposed program for ground observations of a trail of triethyl boron is very similar to the standard program which is used on trails of trimethyl aluminum. The program consists of two types of observations for which adequate field personnel were provided.

III. ORIGINAL EXPERIMENTAL DESIGN

A. Photometer

1. <u>Photometer Requirements.</u> — The photometer located in the nose of the Apache measures vertical integrated oxygen emission (5577Å) as the payload rises through the altitude region. From these measurements an altitude distribution of the oxygen emission can be obtained and correlated with the glow of TEB when it is released on the down trail. To make these measurements, the photometer must be capable of measuring a maximum of 400 Rayleighs when it is below the lower limit of the emission layer ~79 kms and obtain at least 10 measurements as it passes through the oxygen layer approximately 30 km thick. Since its integrated signal as measured from the ground has shown variation from 60 to 500 Rayleighs, it is estimated that a dynamic range of 5 to 500 Rayleighs is required for a successful experiment. The design problem, therefore, is one of optimizing the following design factors: (1) largest aperture consistent with Apache payload, (2) largest field-of-view consistent with the optical pass band, (3) narrowest optical pass band available in an interference filter, and (4) minimum dark current at maximum gain in a photomultiplier tube. It is believed that the photometer design, Table 2, represents the limit of the state-of-the-art for this rocket payload. The low level capability requirement is a result of the desire to measure those signals near the top of the oxygen layer with a reasonable signal to noise ratio. From a typical flight profile, Figure 2, it is apparent that there will be only 25 seconds available for these measurements beginning with the nose cone ejection and ending at an altitude of 110 km. Also shown on the figure is an integrated set of measurements beginning with a 200 Rayleigh signal. For this example, the flight through the layer would last approximately 13 seconds. With an instrument capability of one data point per second there will be approximately 13 points to define the curve from 90 km to 110 km, providing measurement can be made to a level of 10 Rayleighs. Should the initial integrated signal be lower, the number of significant data points will be reduced accordingly.

   a. <u>Signal-to-Noise Ratio.</u> — The signal-to-noise ratio of the instrument is given by the equation:

$$\frac{S}{N} = \frac{\theta_s \sqrt{t}}{\sqrt{\theta_s + \theta_b}}$$

where θ_s is the photocathode electrons per second produced by the signal, t is the time constant of the instrument in seconds, and θ_b is the photocathode electrons per second produced by the background. In terms of the instrument parameters

TABLE 2

SPECIFICATION FOR ROCKET PHOTOMETER

|	
Aperture	2.50-inches diameter
Focal length	6 inches
Optical bandwidth (at 5577$\overset{\circ}{A}$)	1/2 width: 4.5$\overset{\circ}{A}$ 1/100 width: 9.0$\overset{\circ}{A}$
Field-of-view	5° total angle
Baffling	Sunlight reduced by more than 10^5 for angles greater than 15 degrees from optic axis
Photocathode	S-20 surface
Time constant of electronics	1/20 second
Output	3 channels with relative gains of 1, 10, 100 and ~10 percent overlap conditioned to read between 0 to 5 volts
Wavelength scanning (typical at 5577$\overset{\circ}{A}$)	adjustable tilt, 8$\overset{\circ}{A}$ with 6 degrees tilt angle 1/2-sec duration on each position
Rocket vehicle	Nike Apache
Sensitivity (typical at 5577$\overset{\circ}{A}$)	10 Rayleigh signal in 200 Rayleigh/$\overset{\circ}{A}$ background Threshold signal ~10 Rayleigh (dark current limited)
Weight	12 pounds
Power	0.5 watts at 28 volts (without heaters)
Size	6-inches diameter by 16-inches long
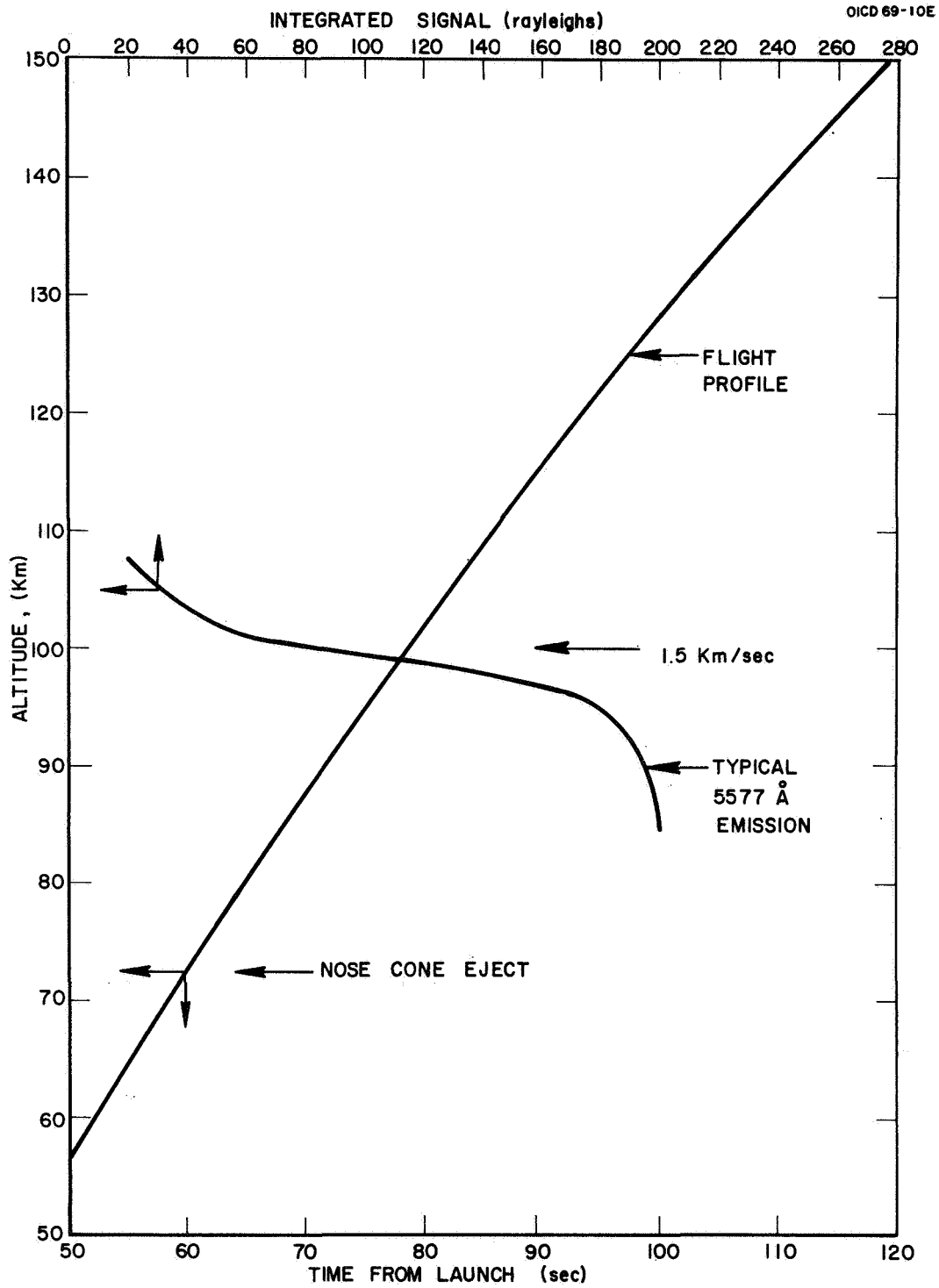
Figure 2. Typical flight profile and integrated 5577Å emission.

$$\frac{S}{N} = 10^6\, R \left(\frac{A\ T\ \Omega\ k\ h\ c\ t}{10^6\ R\ h\ c\ +\ E\ T\ W\ \lambda} \right)^{\frac{1}{2}}$$

where R = signal strength (Rayleighs)

A = instrument aperture (31.65 cm^2)

Ω = field-of-view - steradians (5.96 x 10^{-3} ster)

T = transmission (0.2)

k = photocathode quantum efficiency 0.09

h = Plancks constant 6.625 x 10^{-27} erg sec

c = speed of light 3 x 10^{10} cm/sec

t = time constant (sec) 1/20 sec

E = background radiance (ergs/cm^2-sec ster $\overset{o}{A}$)

W = bandwidth of the interference filter ($\overset{o}{A}$)

λ = wavelength of interest 5.577 x 10^{-5} cm

Using the instrument parameters listed in Table 1, the (S/N) ratio for the expected extreme values of signal and background are:

5577$\overset{o}{A}$ Radiation Rayleighs	Background Radiance ergs/cm^2-sec $\overset{o}{A}$ ster	S/N
200	10^{-6}	185.0
200	10^{-3}	119.0
5	10^{-6}	28.6
5	10^{-3}	3.95

A signal-to-noise of 10 is a reasonable design objective for this type of equipment. The background radiance is that radiance observed at zenith from the ground at solar depression angles of 18 and 7 degrees respectively. These values are not expected to change appreciably as most of the radiation that is seen at zenith from the ground after 7 degree SDA is originating at about the oxygen layer altitude.

   b. Photomultiplier Tube Selection.— There is a wide range of photomultiplier tubes available to the designer. In this application the size, as determined by the optical system, is approximately 3/4-inch diameter. Of primary importance in the selection of the photomultiplier tube are (1) the environmental specifications (because of the high shock and vibration loadings expected), (2) high quantum efficiency at 5577$\overset{o}{A}$ because of the very low signals to be measured, and (3) low dark current at a gain

12

of 10^6 because dark current should not limit the detection capability and therefore should be less then the background signal.

Previous experience with photomultiplier tubes for similar applications has shown that the EMR tubes will meet all the above requirements. Two types of tubes, the S-11 and S-20, were considered for this application. It was hoped that an S-11 cathode would suffice for the light levels expected because they are much less expensive than the S-20. The problem, however, was the dark current requirement.

For purposes of determining the electronic components required, the photocathode electrons produced by both the signal θ_s and the background θ_b must be calculated. This is done by using the following expressions:

$$\theta_s = \frac{R \times 10^6}{4\pi} \cdot A \, T \, \Omega \, k; \qquad \theta_b = \frac{E \, A \, T \, W \, \lambda \, \Omega \, k}{hc}$$

where all the terms have the same meaning as before. The results are listed below:

Anticipated Oxygen Signals R(Rayleighs)	Anticipated Background Signals $E(ergs/cm^2 \overset{o}{A}$ sec ster$)$	θ_s (photocathode electrons/sec)	θ_b (photocathode electrons/sec)
200	---	5.4×10^5	---
5	---	1.35×10^4	---
---	10^{-6} (SDA = 18°)	---	4.77×10^3
---	10^{-3} (SDA = 7°)	---	4.77×10^6

The lowest anticipated background is:

$$4.77 \times 10^3 \times 1.6 \times 10^{-19} \times 10^6 = 7.6 \times 10^{-10} \text{ amp}$$

whereas a typical dark current for an S-11 photocathode at 10^6 gain is 2×10^{-9} amps.

Consequently, the typical dark current for the S-11 is approximately 3 times the minimum signal level allowing no margin for minimum background safety factor. Therefore, the S-20 tube with a lower typical dark current of 2×10^{-10} amps at 10^6 gain and somewhat improved quantum efficiency must be used.

2. <u>Photometer Description.</u> — The photometer portion of this payload is shown in Figure 3. It consists of a light baffle, a tilting interference filter, a collecting lens, field stop, photomultiplier tube, high voltage power supply, amplifiers, and solenoids.

a. <u>Light Baffle.</u> — After the nose cone has been released, the light baffles prevent direct sunlight from falling on the entrance window, in this case the intereference filter. Since a twilight flight is contemplated, effective shielding of the sunlight is required along the whole length of the photometer.

The need for shielding of the entrance window can be shown by a comparison of the power reaching the detector from the airglow with that caused by window scatter of direct sunlight. An allowable scattering factor is determined as shown below.

The power reaching the detector from sky scattering,

$$P_s = TN_{\lambda(b)} \; \Omega \; A \; \triangle\lambda \quad \text{watts}$$

where
T = optical system transmission (percent),
$N_{\lambda(b)}$ = the zenith spectral radiance due to solar scattering in the wavelength region of interest at the altitude of operation (watts/cm^2 Å ster),
Ω = the solid angle field-of-view of the instrument (ster),
A = the area of the entrance aperture (cm^2),
$\triangle\lambda$ = the passband of the multilayer filter (Å).

The power reaching the detector from window scattering

$$P_w = T \; N_{\lambda(w)} \; \Omega \; A \; \triangle\lambda \quad \text{watts} .$$

$N_{\lambda(w)}$ is the radiance of the entrance window normal to its surface and due to the scattering of incident sunlight by the window.

Now $N_{\lambda(w)}$ must be determined in terms of the spectral solar irradiance $H_{\lambda(sun)}$ and a scattering factor F for the window. F is the fraction scattered downward into the photometer.

$$N_{\lambda(w)} = \frac{FH_{\lambda(sun)}}{\pi} \; \frac{\text{watts}}{\text{cm}^2 \; \text{ster} \; m\mu}$$

Lambert's law is assumed to apply to the scattering (Ref. 5). Substituting

$$P_w = \frac{TFH_{\lambda(sun)}}{\pi} \; \Omega \; A \; \triangle\lambda \quad ,$$
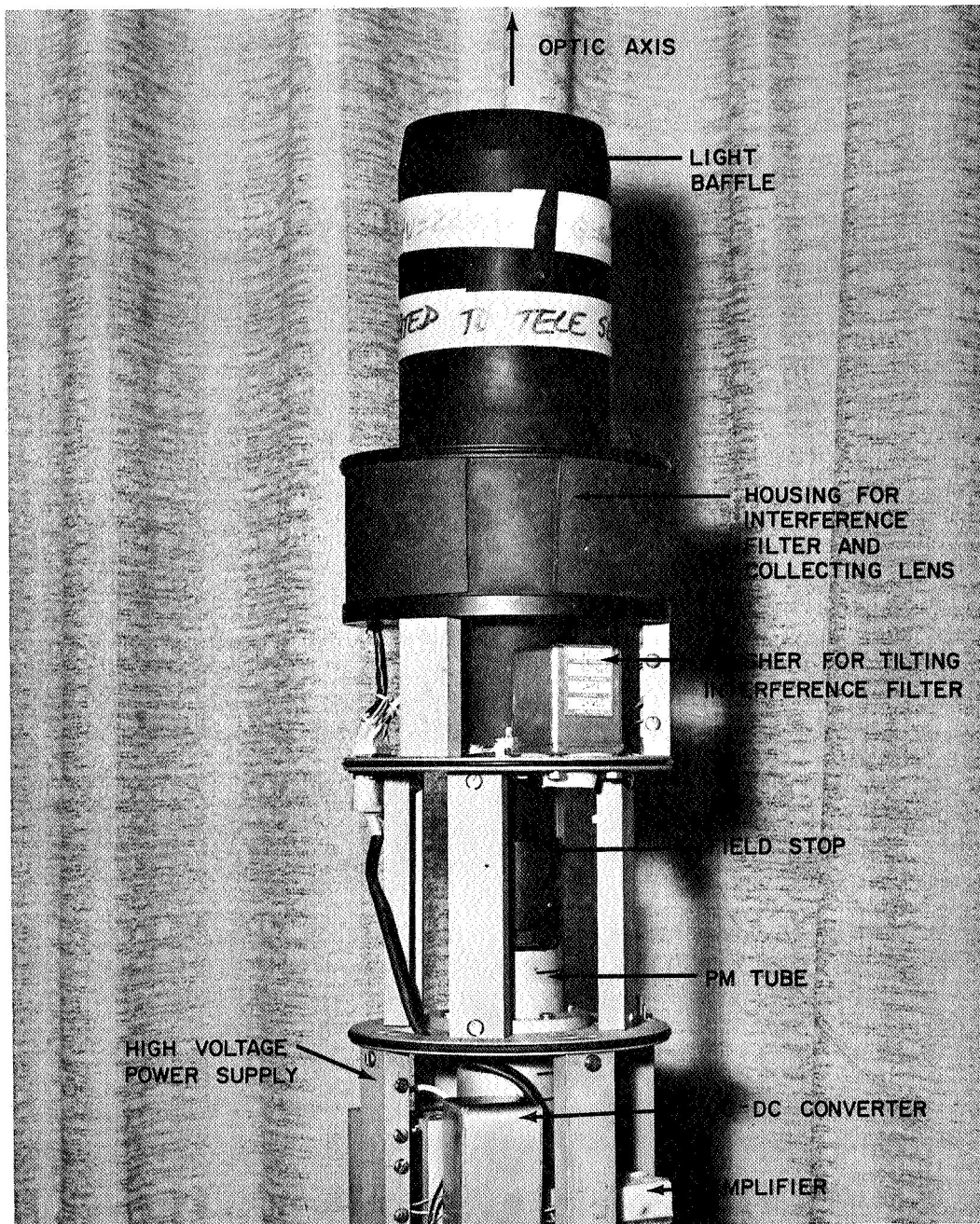
14

Figure 3.   Photometer portion of Apache combined payload.

the ratio of these two power levels can be found from

$$\frac{P_w}{P_s} = \frac{F}{\pi} \frac{H_{\lambda(sun)}}{N_{\lambda(b)}} \quad .$$

As a worst operating condition, the background could be allowed to double by having $P_w = P_s$. Then

$$F = \frac{\pi \, N_{\lambda(b)}}{H_{\lambda(sun)}}$$

the radiance $N_{\lambda(b)}$ given for the 0.5 region and 30-km altitude is 9×10^{-5} watts cm^{-2} ster^{-1} μ^{-1}. At 70,000 ft (21.4 km), the radiance is about three times larger or 2.7×10^{-4}. In terms of $m\mu$, this value would be divided by 10^3 so that

$$N_{\lambda(b)} = 2.7 \times 10^{-7} \frac{watts}{cm^2 \ ster \cdot m\mu} \quad .$$

A value for $H_{\lambda(sun)}$ may be obtained from Handbook of Physics,

$$H_{\lambda(sun)} = 2 \times 10^{-4} \ watts \ cm^{-2} \ m\mu^{-1} \ .$$

Now the scattering factor may be found,

$$F = \pi \frac{2.7 \times 10^{-7}}{2 \times 10^{-4}} = 4.2 \times 10^{-3} \quad .$$

A scattering by the window of 0.4 percent, therefore, reduces the capability of the photometer to measure small signals by two times. A scattering factor of 0.04 percent would be desirable to reduce the loss to a value which would not interfere with most measurements. Such low values are not practical requirements of an unprotected optical surface.

The multiple baffles are therefore necessary to keep direct and reflected sunlight from the first optical surface.

An ideal light baffle is one which allows only those light rays of interest to pass into the photometer aperture. It is possible to make an ideal baffle in the following manner. Into the walls of a conical tube are cut grooves which are perpendicular to the optical axis of the

16

instrument. If the depth of the grooves is large in comparison with the width, the light entering the groove even at high angles will rebound many times before being re-emitted and if the reflectivity of the surface is low, the intensity of the re-emitted light beam will be reduced by approximately 10^3 at each groove. The edges of the groove must be as sharp as possible in order that as little light as possible is reflected from them.

A light baffle was constructed such that a light ray entering the system at greater than 75 degrees to the optic axis will be reflected away from the photometer. For angles between 75 and 15 degrees, some light will be reflected inward. If the reflectivity of each surface is 0.01, the incident light beam will be reduced by 4 orders of magnitude by each groove that it enters. It is estimated that the baffle arrangement which is 5.6-inches long will effectively remove incoming sunlight which has angles larger than 75 degrees with respect to the optic axis and attenuated that which is between 75 and 15 degrees by a factor of 10^5.

b. <u>Objective Lens.</u> — The lens is a plano-convex lens with an f ratio of 1.63 and is used to gather the light and deliver it to the photocathode. The field stop determines the circular field-of-view which for this radiometer is 5-degrees total angle.

c. <u>Interference Filter.</u> — The interference filter has the following specfifications:

(1) Maximum overall diameter: 2.875 inches

(2) Minimum usable aperture: 2.500 inches

(3) Peak wavelength at 0-degree incidence: 5585Å

(4) Half width: Not greater than 3Å

(5) 1/100 width: Not greater than 9Å — this will insure that the filter as used in the field-of-view will have its low wavelength 1-percent transmission point at 5579Å.

(6) Effective index of refraction: 1.45

(7) Transmission: A minimum of 35 percent at peak wavelength

(8) The filter will be blocked to a wavelength of 1 micron.

The interference filter is mounted in a cassette which in turn is mechanically attached to a solenoid. The solenoid drives the interference filter between two positions 6-degrees apart. This allows the photometer to "look" at first background and then background plus oxygen radiation at 0.5-second intervals, that is, one data point per second.

d. <u>Preamplifier Design.</u> — The design of the preamplifier will depend on PMT dynamic range and information bandwidth requirements. Scaling of the PMT anode current by means of PMT gain setting will be determined primarily by the maximum permissible anode current consistent with stable operation.

Calculations of required dynamic range for the 7-degree SDA design and the 18-degree SDA design have been developed to provide optimum performance in each case. These dynamic ranges were then extended to give reasonable margins of safety for both signal and background levels.

At 7-degree SDA

Background: Calculated level - 5×10^6 photocathode electrons/sec
Range provided - 5×10^5 to 5×10^7 photocathode electrons/sec

Signal: Calculated maximum level - 10^6 photocathode electrons/sec
Extension provided - 10^7 photocathode electrons/sec

Lower Limit (lowest background and no signal): 5×10^5 photocathode electrons/sec

Upper Limit (highest background plus extended signal level): 6×10^7 photocathode electrons/sec

Dynamic Range: approximately 2 decades: 5×10^5 to 6×10^7 photocathode electrons/sec

At 18-degree SDA

Background: Calculated level - 5×10^3 photocathode electrons/sec
Range provided - 2.5×10^3 to 5×10^4 photocathode electrons/sec

Signal: Calculated maximum level - 10^6 photocathode electrons/sec
Extension provided - 2.5×10^6 photocathode electrons/sec

Lower Limit (lowest background and no signal): 2.5×10^3 photocathode electrons/sec

Upper Limit (highest background plus extended signal level): 2.5×10^3 photocathode electrons/sec. Highest background insignificant compared to maximum signal.

Dynamic Range: 3 decades; 2.5×10^3 to 2.5×10^6 photocathode electrons/sec

Maximum anode current will tentatively be limited to 4×10^{-6} amps for reasons of aging and stability characteristics. PMT gain will be adjusted with that as a limiting condition.

At 7-degree SDA

Maximum anode current (given) = 4×10^{-6} amps

$$\text{Gain} = \frac{4 \times 10^{-6}}{6 \times 10^7} (6.25 \times 10^{18})$$

$$= 4.17 \times 10^5$$

18

$$\text{Minimum anode current} = \frac{(4.17 \times 10^5)(5 \times 10^5)}{6.25 \times 10^{18}}$$

$$= 3.33 \times 10^{-8} \text{ amps pk}$$

At 18-degree SDA

Maximum anode current (given) $= 4 \times 10^{-6}$ amps

$$\text{Gain} = \frac{4 \times 10^{-6}(6.25 \times 10^{18})}{2.5 \times 10^6}$$

$$= 10^7$$

$$\text{Minimum anode current} = \frac{10^7(2.5 \times 10^3)}{6.25 \times 10^{18}}$$

$$= 0.4 \times 10^{-8}$$

$$= 4 \times 10^{-9} \text{ amps pk}$$

At the preamplifier input, a load resistor value will be computed to satisfy bandwidth requirements.

$$R_L = \frac{1}{2\pi(BW)C}$$

where   BW(3 dB) = 400 cps

C = 100 pf typical

$$R_L = \frac{1}{(6.28)(4 \times 10^2)(10^{-10})} = \frac{10^8}{25}$$

$$R_L = 4 \times 10^6 \text{ ohms maximum .}$$

Actually, to obtain a margin of safety and also to optimize subsequent scaling, an R_L of 10^6 ohms was selected.

Preamp input voltages developed across $R_L = 10^6$ ohms are:

At 7-degree SDA

$$e_{\text{max pk}} = (4 \times 10^{-6})$$

$$= 4.0 \text{ volts}$$

$$e_{min} = (3.33 \times 10^{-8})(10^{6})$$

$$= 3.33 \times 10^{-2} \text{ volts}$$

Dynamic range: 2 decades

At 18-degree SDA

$$e_{max \ pk} = 4.0 \text{ volts}$$

$$e_{min} = (4 \times 10^{-9})$$

$$= 4 \times 10^{-3} \text{ volts}$$

Dynamic range: 3 decades

If the preamplifier is of unity gain, the same voltages will appear at the preamplifier output for scaling to meet telemetry requirements over the dynamic range.

e. Range Scaling. — In order to handle a maximum of 3 decades range three full-time telemetry channels of btter than 400-cps bandwidth were used and a fourth or fifth channel carried the signal from the monitored high voltage and filter position.

Each channel operated simultaneously; and cascaded such that each channel handled one decade plus a reasonable overlap of range at both ends of that decade. In block form, the signal circuits are shown as below:

20
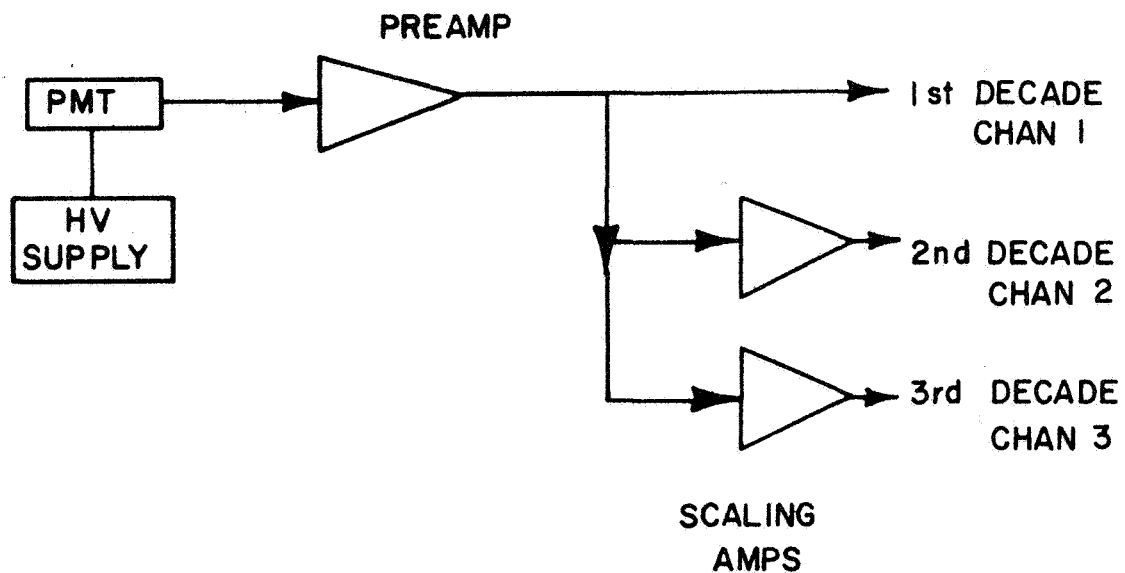
Allowing for overlapping ranges and a 0 to +5-volt limiting telemetry input requirement, the following table of voltage levels were used.

	Preamp Input/Output	Scaling Amp Gain	Output to Telemetry
1st decade	4 mV to 40 mV	100	0.4 to 4 V
2nd decade	40 mV to 0.4 V	10	0.4 to 4 V
3rd decade	0.4 V to 4 V	1	0.4 to 4 V

Typical telemetry channel accuracy and resolution is 1 percent of full scale (5 volts) which is 0.05 volts. In this design, a scale range of only 3.6 volts is used to allow overlap and resolution. The resolution obtained within the 3.6-volt range is:

$$\frac{0.05}{3.6} = \frac{1}{72} = 1.4\text{-percent resolution}$$

an overlap of 0 to 0.4 volts is reserved at the low end which is:

$$\frac{0.4}{0.05} = 8 \text{ percent under range margin}$$

and an overlap of 4 to 5 volts is reserved at the high end which is:

$$\frac{1}{0.05} = 20 \text{ percent over range margin .}$$

3. Preflight Tests

a. <u>Twilight Observations and Preflight Tests.</u> — In order to obtain the maximum voltage reading while observing radiation at $\lambda5577\text{Å}$ from the ground, the electrical gains of the photomultiplier tube and the amplifiers were set so that the instrument was actually dark-current limited. Under these conditions the output voltages normalized to the most sensitive were:

Payload No.	Oxygen plus Background	Background	Dark Current	Calibration
14.283	11.0 volts	4.0 volts	1.10 volts	28.2 Rayleigh/volt Å
14.284	4.8 volts	2.0 volts	0.27 volts	70 Rayleigh/volt Å

Both photometers were calibrated using a tungsten-iodine (Ref. 5) source. The calibration factors are given above. During a night sky observation prior to flight the photometers measured approximately 200 Rayleighs of atomic oxygen emission.

The two photometers were taken to Goddard Space Flight Center for vibration tests. After these tests, a number of welded joints were broken, presumably due to poor penetration during the welding operation. This problem was rectified by fastening the pieces together with No. 8-32 screws. Other than this, no other mechanical or electrical problem could be detected, within the photometer section.

A copy of the horizontal and vertical checks is given in Table 3. A light source mounted in the nose tip provided signals which were monitored at the telemetry station. No variation in these signals was seen between the horizontal and vertical positions. The only variation of signal strength was caused by floodlights being turned on for photography.

TABLE 3

VERTICAL AND HORIZONTAL TESTS

1. Instrumentation on and +4.5-volt supply on at monitor ignition, Batteries No. 1 and No. 2 at console.
2. Photometer on.
3. Start Chart Recorders, Channels 13 to 18 at 2 inches/sec.
4. Xmtr on at 231.4 MHz.
5. Filter on.
6. Filter off.
7. Photometer off.
8. Photometer on.
9. High voltage off.
10. High voltage on.
11. Internal power.
12. Filter on.
13. Filter off.
14. External power.
15. Photometer off.
16. Photometer on.
17. Xmtr off.
18. Photometer off.
19. Recorders off.
20. Instrumentation off.

B. Payload Design

The first model of the combined TEB-photometer payloads which were designed and fabricated are shown schematically in Figure 4.

The split nose cone is designed to provide the proper aerodynamic shape and to protect the photometer from ram air pressure blast and heating effects as well as to provide a light-tight covering during the initial portion of the flight. These requirements were met by machining the nose cone from separate castings which had been thermally stabilized so that they would not warp during environmental testing and pre-flight handling. After final assembly, the light-tightness was checked and was found to be far more than adequate, so much so in fact that the inside of the nose cone did not have to be painted black as is the normal requirement for an instrument of this nature.

At approximately 50 seconds after launch at an altitude of about 60 kilometers, the controls in the instrumentation section fire the ejection mechanism which is located at the base of the nose cone. This ejection mechanism releases the nose cone from the top of the payload shell and allows the two halves to rotate about the nose tip and then separate, thus completely exposing the photometer and allowing it to operate. Prior to this operation the photometer is calibrated continuously during flight by a small light source which is fastened to one of the nose cone halves within the field-of-view of the photometer. The removal of this light source gives an easily identifiable signal to the photometer and thus is an indication that the nose cone has indeed been ejected. Therefore, no separate monitor is provided. By unlatching the split nose cone from the bottom and allowing it to rotate about its tip, the rather common phenomenon of vehicle slow-down in rotation is avoided. The alternative technique of nose cone removal is to unlatch the nose cone at the top and to allow it to rotate about the bottom. This is mechanically simpler than the design chosen, however, it can reduce the payload spin by as much as 50 percent thus reducing its gyroscopic stability and may induce a considerable coning angle. Since the photometer is making an integrated measurement of the O layer, it is desired to have as small a coning angle as possible, and therefore, the tip release nose cone would be unsuitable. In addition, it is almost impossible to make a tip release design light-tight which would add further complications. The release mechanism employed is adapted from similar units used by GCA on many other payloads and has proved to be highly reliable.

The instrumentation section contains the controls, aspect sensor, power supplies, telemetry system, battery power supplies and timing systems. It was decided that, in view of the many interrelated functions, two complete redundant timing systems should be used. Inasmuch as all of the pyrotechnic devices are dual bridge units, one bridge of each device is connected to each timing deck, as shown schematically in Figure 5, thus giving complete
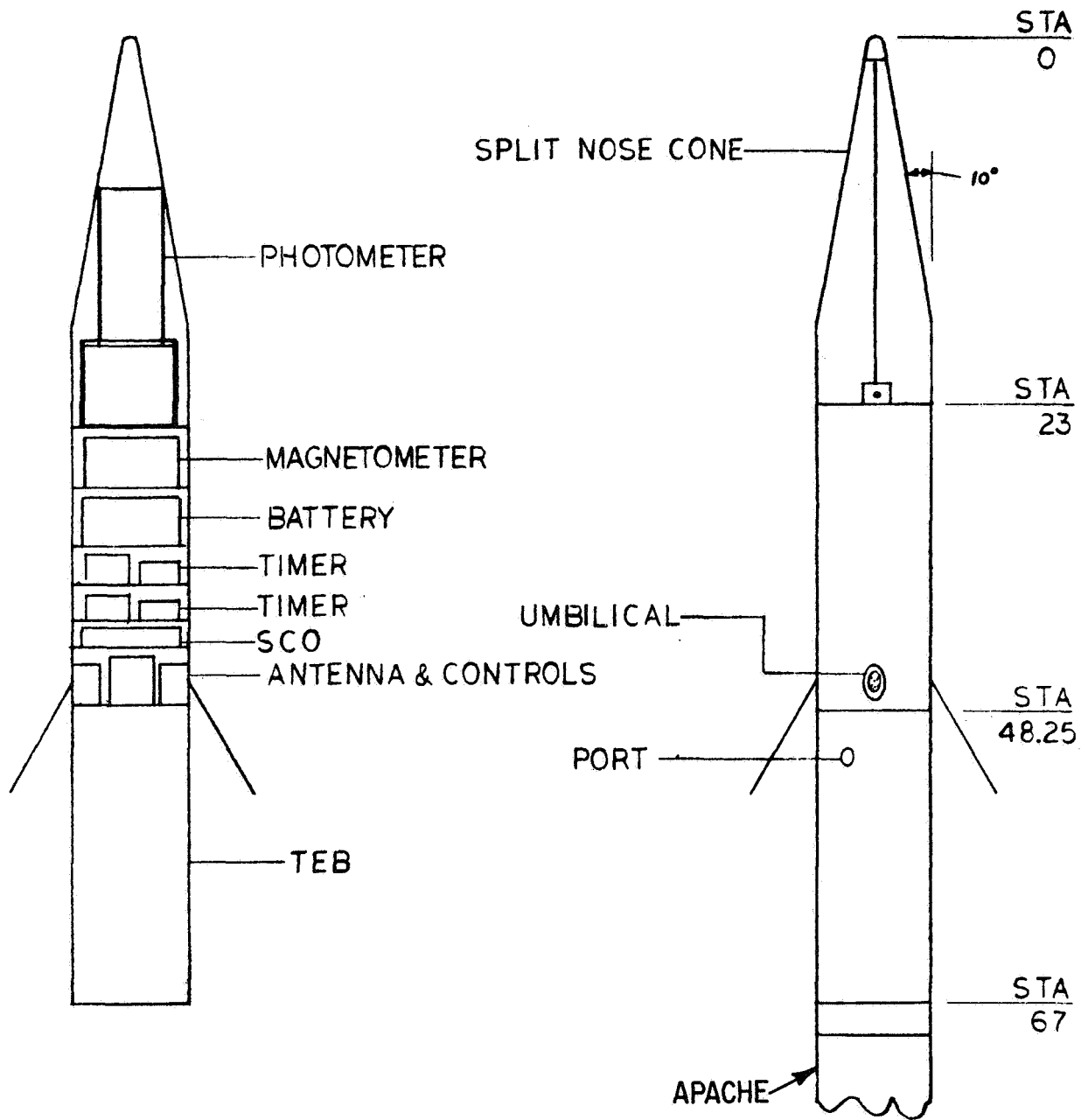
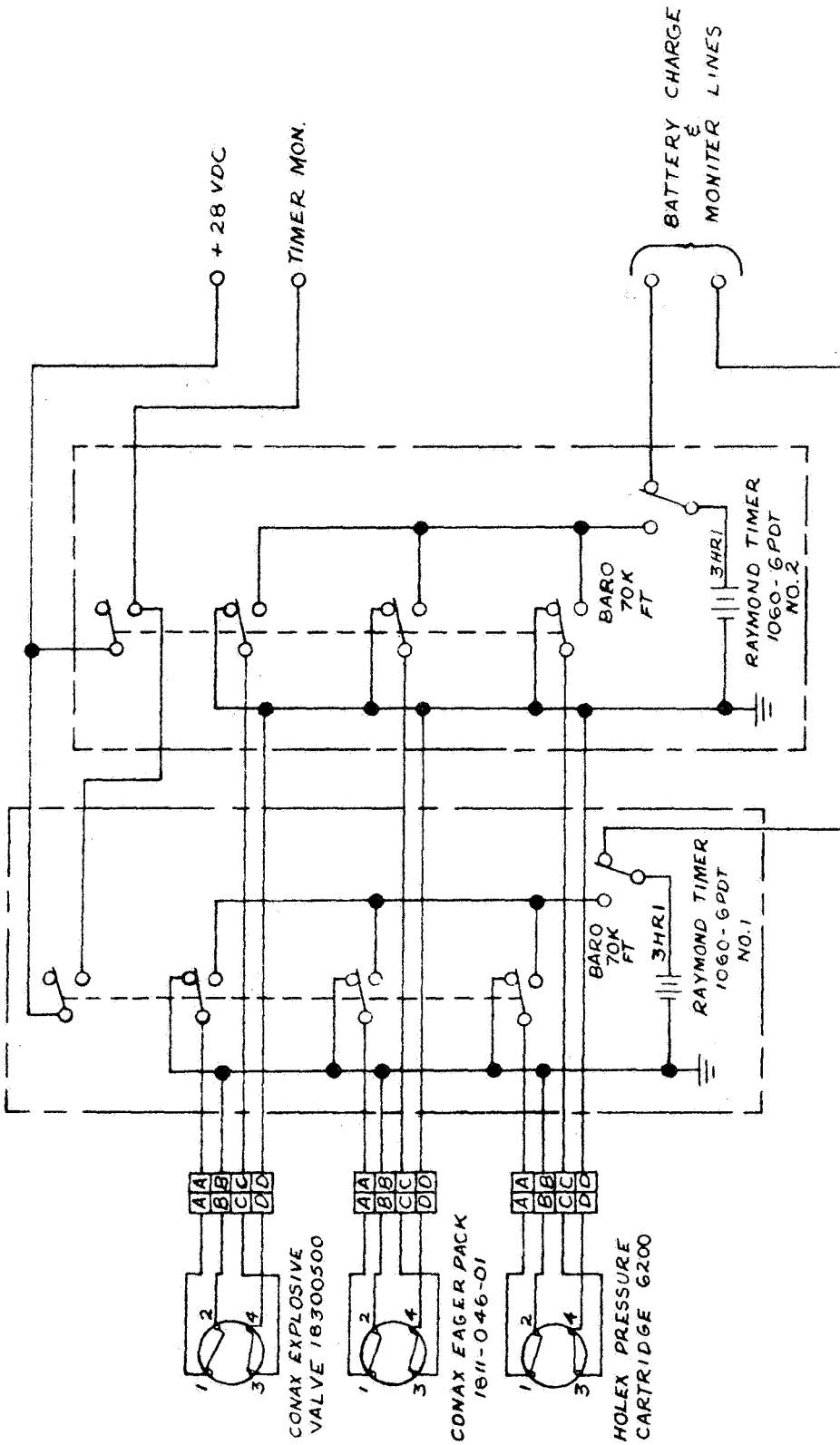Figure 4. Combined TEB photometer payloads.

Figure 5. Firing circuit combined payload photometer/TEB.

25

redundance to each pyrotechnic and timing function. The timer decks are shown schematically in Figure 6. The timing function is initiated by a baroswitch which performs several functions. On the ground this baroswitch connects the ignition battery to the ground charging system, thus providing a positive indication of system safety as well as allowing the ignition battery to be charged to discharged. The ignition battery system consists of three Yardney HR-1 cells which give a nominal output of 4.5 volts. This system is used rather than the normal "hot" battery to comply with Wallops Island Range Safety Requirements even though it does add some complexity to the system. However, the additional safety to personnel which is obtained by positive knowledge that the ignition battery cannot fire the pyrotechnics is considered to be worthwhile. At approximately 28 seconds after launch the baroswitch closes and fires squib dimple motors which start the Raymond Model 1060 timer, thus initiating the timing sequence. This sequence is as follows (as set in the field):

T + 34 - photometer filter is released

T + 50 - nose cone is ejected

T + 166- heater is turned on

T + 226- TEB is released

T + 400 (approx.) - impact.

The magnetometer is a magnetic aspect sensor, Schonstead Model RAM-3 which is encased in a protective can is a configuration which has been used many times. The main battery power supply consists of Yardney PM-3 cells in an aluminum container in a configuration which also has been successfully flown. The telemetry system is mounted on the bottom two decks of the instrumentation section and consists of subcarrier oscillators, a mixer amplifier, transmitter, and turnstile antennas. The subcarrier oscillator frequency assignments are as follows:

(1) Channel 19 (70 kHz, 7-1/2 percent deviation) Photometer signal Channel 1.

(2) Channel 17 (52.5 kHz, 7-1/2 percent deviation) Photometer signal Channel 2.

(3) Channel 16 (40 kHz, 7-1/2 percent deviation) Photometer signal Channel 3.

(4) Channel 15 (30 kHz, 7-1/2 percent deviation) Sync monitor.

(5) Channel 14 (22 kHz, 7-1/2 percent deviation) H.V. monitor.

(6) Channel 13 (14.5 kHz, 7-1/2 percent deviation) Magnetic Aspect Sensor and Baroswitch Monitor.

These same two decks also contain the umbilical connector and control relays which are operated from the ground.
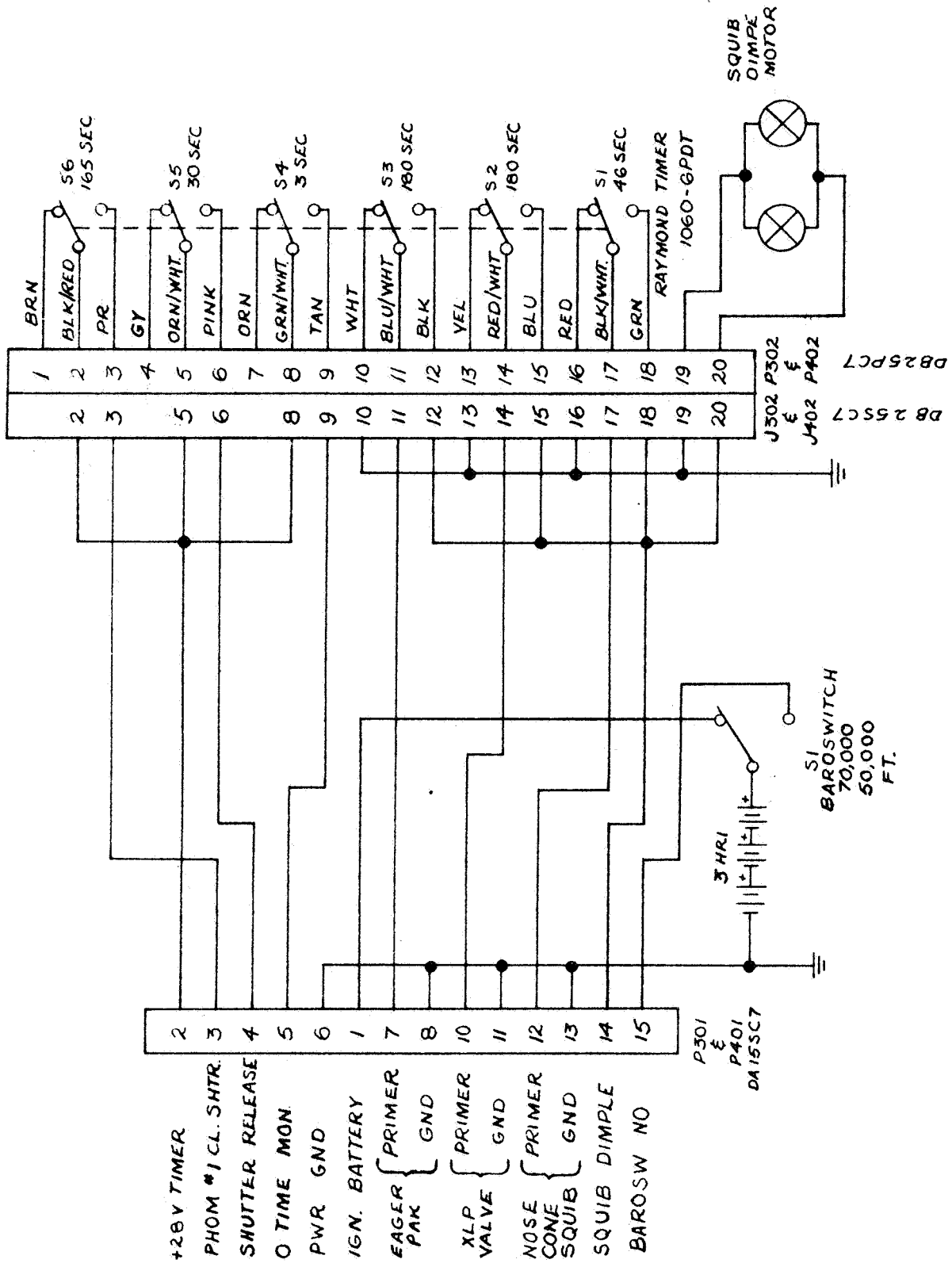
Figure 6. Schematic timer deck.

27

The triethylboron module is essentially identical to the TMA modules which GCA has flown in the past. The triethylboron (TEB) is contained within a teflon bladder inside the canister. This bladder is filled by the TEB manufacturer at his plant and the container remains sealed until the moment of intended release in flight. At that time the timers initiate explosive values which allow the TEB to be forced from the bladder under pressure from a nitrogen bottle.

The total payload weight is 68 pounds, and the payload length is 67 inches. This combination produces a payload which is inherently stable and thus minimizes coning and aerodynamic loading on the joints. The apogee altitude will be 160 kilometers and the time to apogee, 200 seconds.

The two payloads constructed in the program were taken to NASA/Goddard for environmental testing on Tuesday, March 21. Telemetry was checked out on 22 March, and the payloads subjected to vibration in all three axes on 23 and 24 March. After conclusion of vibration testing the payloads were checked functionally including blowing a nose cone and recheck of the telemetry. In one case a timer connector was damaged and had to be replaced. This was of a relatively minor nature and was corrected at Goddard. Even with these discrepancies the payloads were completely operable and showed no electrical malfunctions.

The payloads were taken to the Wallops Island launch site on Saturday, March 25, and the photometer and the rest of the payloads were checked out on a continuous basis from then until the day of the actual flight. On Monday, March 27, the payloads were made ready for the flight which occurred Thursday, March 30.

The flight was not successful, and the information available seems to indicate that telemetry failed and that possibly TEB does not chemiluminence or was not released. A ground test of the second payload was performed on Friday, March 31. The payload operated perfectly in this ground test. The analysis of the flight failure is given in Section IV. See Figure 7 for successful ejection of TEB in ground test.
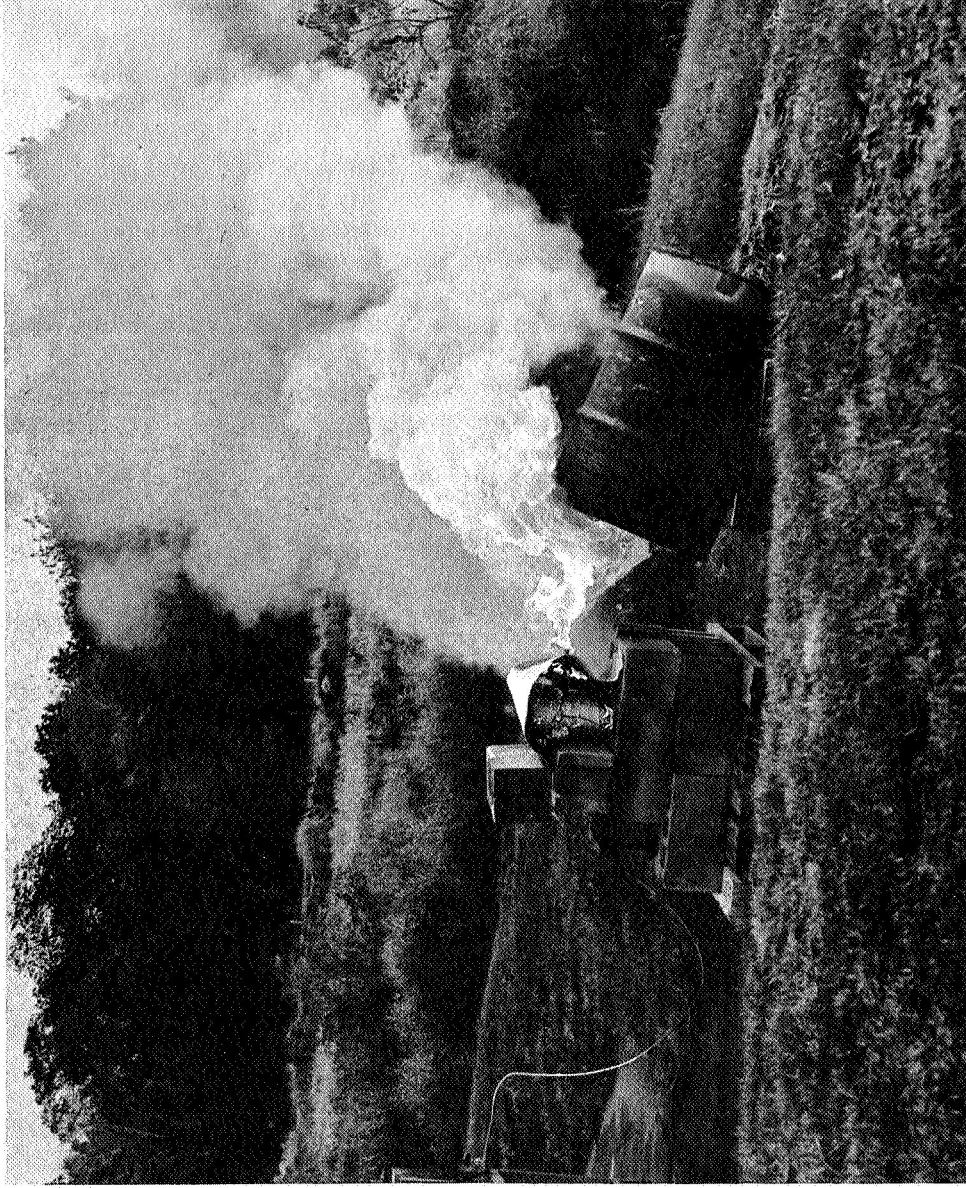
Figure 7. Field demonstration of TEB canister successful operation.

IV. SUMMARY OF POST-FIRING DIAGNOSIS
OF 30 MARCH 1967 ROCKET LAUNCH

In view of the failure of the first payload, it was necessary that a failure analysis of this payload be performed before any similar payloads were flown in the future. In the engineering of a payload one can set out a chain of events running from input of the experimental requirements through design, fabrication, assembly, test, and then actual flight. In a failure analysis program, each step is to some extent dependent on the results of the preceding step as to the direction on which it will take. In this case, this is especially so since the payload in unobtainable for scrutiny. The information available can be summed up as follows. First, the transmitted signal from the telemetry system decreased markedly in output at approximately NIKE burnout. Second, the nose cone came off on schedule as confirmed both by internal data and external radar observation. Third, no chemiluminescence was seen. Fourth, during that short portion of the flight where signals from the aspect magnetometer were readable, there does not appear to be any unusual motional effect nor is there anything unusual from the radar plot; this behavior indicates that no malfunction of the motors had occurred.

The most obvious answer to the observed loss of signal at NIKE burnout is that the transmitter failed since the failure mode and time are almost identical with other failures experienced with payloads using the same type of transmitter, Vector TRPT-250. It is our understanding that the defects attributed to the transmitter which were observed at that time have been corrected by the manufacturer. In view of the efforts by the manufacturer after the last series of failures, it is possible that the transmitter operated satisfactorily, and the fault may lie in some other area. The failure has already been discussed with the manufacturer who is conducting tests. If, of instance, the harness wires were to become strained and experience a small fracture such that the ends were still relatively close to one another, the signal could still reach the antennas by capacitive coupling across the gap in the wire. This would be equivalent to putting a high impedance in series with the antennas and thus could conceivably account for the large reduction in gain. A failure of this nature could occur anywhere between the output of the transmitter and the actual connection to the antenna. Therefore insofar as the transmitter is concerned, failure analysis would have to proceed on at least two levels simultaneously, the first with the manufacturer of the transmitter and the second with the arrangement and construction of the antenna and harness system.

The apparent cause for failure of the chemical release appears much more difficult to establish. It is known that the nose cone released on schedule and that the photometer appeared to be operating properly at this time. Therefore, at least one timing module was operating properly, and there should have been sufficient power to operate the remaining pyrotechnic

devices, together with the successful ground tests conducted at NASA/Wallops, make it seem highly unlikely that one of these devices failed to operate.

In view of the above it is far more likely that some non-pyrotechnic device failed or that some interaction occurred which caused the failure of the chemical release section. A possible candidate for a device failure is the regulator-hose combination which feeds the compressed nitrogen into the cavity surrounding the teflon bladder. These regulators are special items and therefore do not have the built-in reliability of the pyrotechnic units which are mass produced and have been extensively tested. If the regulator should fail, the hose will see almost four times the rated burst pressure and would fail almost constantly.

V. PAYLOAD REDESIGN AND FABRICATION

A. General

The overall design of the payload was reviewed in order to modularize the subsystems as well as the component parts within them. This resulted in much improved testing and servicing of each subsystem on an independent basis. The TEB subsystem contains its own timers, batteries and umbilical connection. The photometer subsystem contains its own timer for unlatching the interference filter after launch. The photometer and telemetry subsystem, however, do share 28-volt batteries, but this is no problem when the subsystems are separated since power supplies are readily used. Finally the nose-cone subsystem has a self-contained baroswitch, timer, battery pack and release mechanism for independent control and operation.

Component parts in each of the subsystems are mounted in rack and panel fashion wherever possible using a mechanical framework of rails and decks to support all parts and wiring. Where corona protection is required under the PMT and high voltage power supply, an aluminum housing is provided under the deck to facilitate shielding and potting. The backup payload which has been retained from the previous tests was dismantled and reassembled on the new modular frame to take advantage of the improved accessibility. Specific changes and improvements in each subsystem will be described in the following sections.

B. Photometer Subsystem

The revised functional block diagram of the photometer is shown in Figure 8. The system design is basically unchanged from that described in Section III.A. In this case, however, an electrometer preamplifier converts the low level dc PMT current to a voltage proportional to the magnitude of the feedback resistor (2.2 megohms). The voltage represents the first decade of a 3-decade dynamic range of signal output and is designated Channel 1. Two scaling amplifiers are coupled to this output; one scaled to ten times input, the other to 100 times input operating simultaneously with Channel 1 and designated Channels 2 and 3 respectively.

All three channels, covering three contiguous decades independently, drive three standard low bandwidth telemetry channels.

C. Telemetry Subsystem

The telemetry subsystem consisting of the voltage controlled oscillators (VCO's) for all channels, aspect sensor, control relays and main batteries is basically similar to the previous model design. Only one component has been changed due to a repetitive reliability problem.
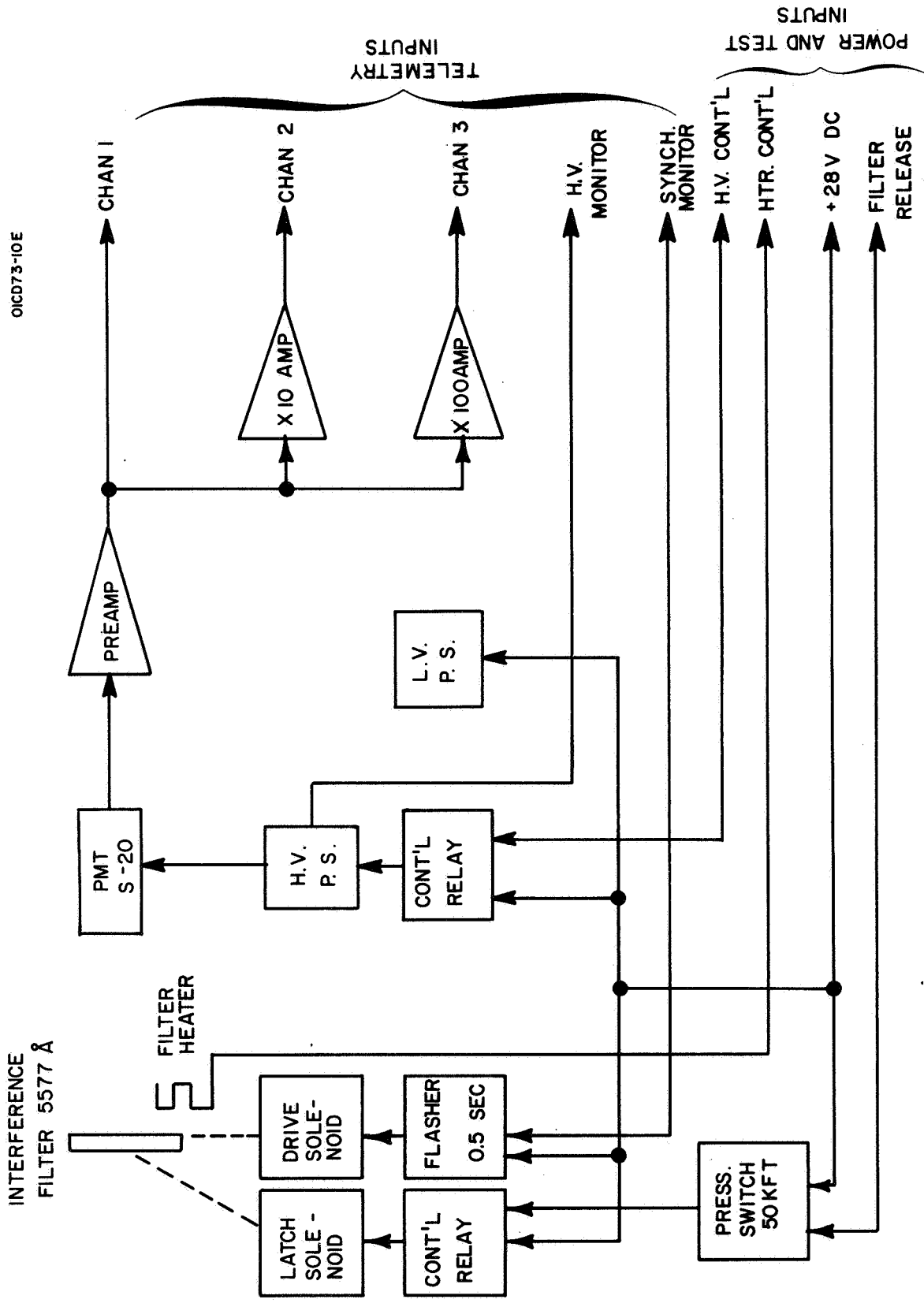
32

Figure 8. Oxygen photometer functional block diagram.

33

The Vector transmitter, Model TRPT-250-RAO has been replaced by a Telemet Model 3008-A1. In view of recent telemetry failures where Vector units had been used, an engineering review of the telemetry requirements was conducted and a decision was made to make the change to the Telemet model.

A few minor wiring and relay control changes were made to improve system servicing facility and to standardize connections with the ground test set through the umbilical cable.

D. Nose-Cone Subsystem

This subsystem was completely redesigned for improved reliability and self-contained operation. A timer, started by a pressure-actuated switch provides sufficient delay after lift-off for safe separation of the nose cone half-sections.

E. TEB Subsystem

Important changes were also made to this subsystem. A test was performed on a TEB canistor to verify ejection by electrically operating the explosive valve. Normal burning of the entire contents was observed to occur. The photograph of Figure 7 shows the burning which took place during the test.

The instrumentation rack for the TEB section was changed so that it is identical with the GCA standard TMA payloads. All of these components, assemblies, and structures have been successfully flown many times. The complete independence of the hazardous TEB subsystem increases safety and efficiency of preparation and launching.

VI. ROCKET FIRING (21-26 FEB.1968) DESCRIPTION, DATA AND CONCLUSIONS

A. General Description

Two combined payloads were assembled, tested and transported to Wallops Island for launch during February 1968. It was planned that one launch should occur during evening twilight and the second a few hours later when nighttime conditions prevailed. Five other vapor trails combined with Langmuir probes were to be spaced throughout the remainder of the night.

All prelaunch checks were completed on schedule and the evening twilight payload was launched on NASA 14.284 CA at 1817 EST on 21 Feb. 1968. The rocket performed well, attaining the predicted altitude of slightly over 15 km during a stable flight. Telemetry and nose-cone separation were as predicted and a trail of TEB was ejected from near the peak of the trajectory to below 90 km. The trail was bright and green in color as compared to the blue visual appearance of TMA during twilight. Good triangulation photographs were obtained from a measurement of upper winds and spectral observations with a spectrophotometer were made in order to assess the value of such observations for the determination of temperature of the neutral atmosphere. The trail did not have the bright, white appearance around 100 km which is characteristic of TMA trail. See Figure 9.

The only unsuccessful portion of the flight involved the airglow photometer. A background signal of unexpected large magnitude occurred throughout the region where measurements were desired. A small amount of high voltage breakdown was observed in this instrument at lower altitudes, but this effect had decayed well before the measurement region. The high background signal did not have the character of voltage breakdown and may have been due to a glow in the bow shock ahead of the photometer. In any event, since the cause was not ascertained at that time, the second launching was postponed to allow further investigation of the possibility of voltage breakdown within the photometer.

All preflight tests on the second instrument were accomplished on schedule as had been done with the first. It was surmised that the photo-tube housing might be restricting the outflow of air during ascent to such a degree that the normal arc-over region was greatly extended. This housing was designed to prevent light leaks to the phototube and also to aid in temperature stabilization of the interference filter. In order to investigate this possibility, the entire photometer was placed in a bell jar vacuum system at Wallops Island and pumped down at various rates. The results verified previous tests and flight experience, i.e. a nominal amount of discharge occurred but subsided quickly. This procedure was repeated after the phototube housing was vented with holes strategically placed to maintain light proof integrity of the system. The results were the same as before. The tests gave no evidence to suspect difficulties in flight; however, similar results had been previously obtained on the first instrument.

Figure 9. Trail of twilight TEB release.

It was decided that the problem could be avoided in the second flight by turning the high voltage off while traversing the critical altitude range and then back on before the region of observation was reached. Only slight modifications were required in order to have the baroswitch turn the high voltage off at an altitude of 50,000 feet and to add a simple electronic timer to turn it back on after the critical region was passed. The solution allowed the operation of the instrument to be monitored throughout powered flight to assure that no damage occurred. The timer used the same circuit and components as employed in the nose-tip release and thus was a pretested unit. The indicated modifications were made and appropriate tests were performed in the vacuum system. The results were as expected; the baroswitch disconnected the high voltage just as the discharge was beginning to be noticeable.

The second payload was flown on NASA 14.350 CA which was launched at 2010 EST on 26 February 1968. Again the rocket, telemetry and nose-tip ejection performed as predicted. The high voltage was turned off by the baroswitch as the high voltage discharge was beginning and was turned on 29 seconds later at 65 km by the preset timer. The photometer was operating and accurately recorded the altitude variation of the 5577Å radiation while passing through the region of emission. Similar recordings were obtained on the downward portion of the trajectory, but these require corrections for rocket aspect. However, a high level signal was again observed on this flight which also had the characteristics of a glow rather than a voltage breakdown. If this glow indeed originates in the bow shock of a high velocity rocket, it would appear that a major modification in experimental procedure is required.

During the flight the sky was clear over all observation sites, but no chemiluminescent trail was observed visually, photographically, or photometrically. This lack of observable emission suggests that either TEB does not produce an observable chemiluminescent glow at night or that the TEB failed to be ejected from the rocket. Although there was no recorded monitor of the ejection mechanism, the latter possibility appears to be unlikely on the basis of the following arguments. During the past three years over two-dozen TMA trails have been produced with an identical ejection system wherein no failures occurred. No trail from TEB was observed on this flight and none was observed during the night of 30 March 1967. The failure of the system to eject only TEB at night when it successfuly ejected it during twilight and has performed successfully on dozens of TMA releases is highly improbable. This statistical conclusion is verified by the previously cited observation that the twilight TEB trail did not show the bright photochemical emission (around 100 km) that is always present on TMA trails. From this observation alone, it could be expected that emission from TEB would not be bright in that region at night and it must be assumed that it was not.

B. Photometer Data

The photometer began recording the 5577Å airglow radiation as soon as the high voltage was turned on. The high voltage power supply and photometer had stabilized on output channel 3 by T + 73 sec which corresponds to an altitude of 82 km. At that time a constant level of 5577Å radiation was being recorded and continued at the same level until an altitude of 91 km when the recorded level began to drop sharply as the rocket passed through the emitting region. The photometer response is shown in Figure 10. The photometer had previously been calibrated in the laboratory with a standard lamp; on the basis of this calibration, the maximum signal recorded was 100 ± 30 Rayleighs. This is a low level for the (OI) airglow; however, a generally low level had been recorded with a ground-based instrument for a period of several days prior to this flight by Dr. E. R. Manring at North Carolina State University, Rayleigh, North Carolina. Unfortunately, Dr. Manring's observing site was completely covered by clouds during the night of this particular firing so that no direct correlation was available.

The recorded altitude profile of the 5577Å emission is as predicted for a forward looking photometer traveling upward through the layer. An essentially constant brightness was recorded until the lower boundary of the layer was reached and then decreased proportionally to the altitude profile of the emission.

The photometer continued to operate throughout the flight and the ejection of TEB had no apparent effect. This lack of interference from the TEB may be due to the fact that there was no significant glow produced at night. The passage through the airglow layer was recorded on the downward portion of the trajectory also. Unfortunately, the rocket tumbled and overturned while traversing the layer, which action complicated the interpretation of the down-leg records. The orientation of the optical axis was determined from the magnetometer records and the recorded brightness values were divided by the cosine of the zenith angle to normalize them to the zenith direction. The results are shown by the circles in Figure 10. This procedure is of course less accurate that the direct measurement obtained on the way up, but the error appears to be primarily in the uncertainty of the heights of the maximum brightness and of the bottom of the layer. The altitude profile and sharp bottom edge of the layer are accurately verified.

Previous similar observations by others (Ref. 4) had not produced the vertical profile shown in Figure 10. A compilation of such measurements (Ref. 6) is given in Table 4. The total data show that on the average the peak 5577Å intesity occurred 13 km above the lower boundary of the layer. According to Greer and Best (Ref. 6), in these cases, the resulting smooth, rounded bottom edge of the layer which extends to below 80 km is probably not real but is due to instrumental effects. They offer two possible explanations; first, the uncertainties associated with removing the
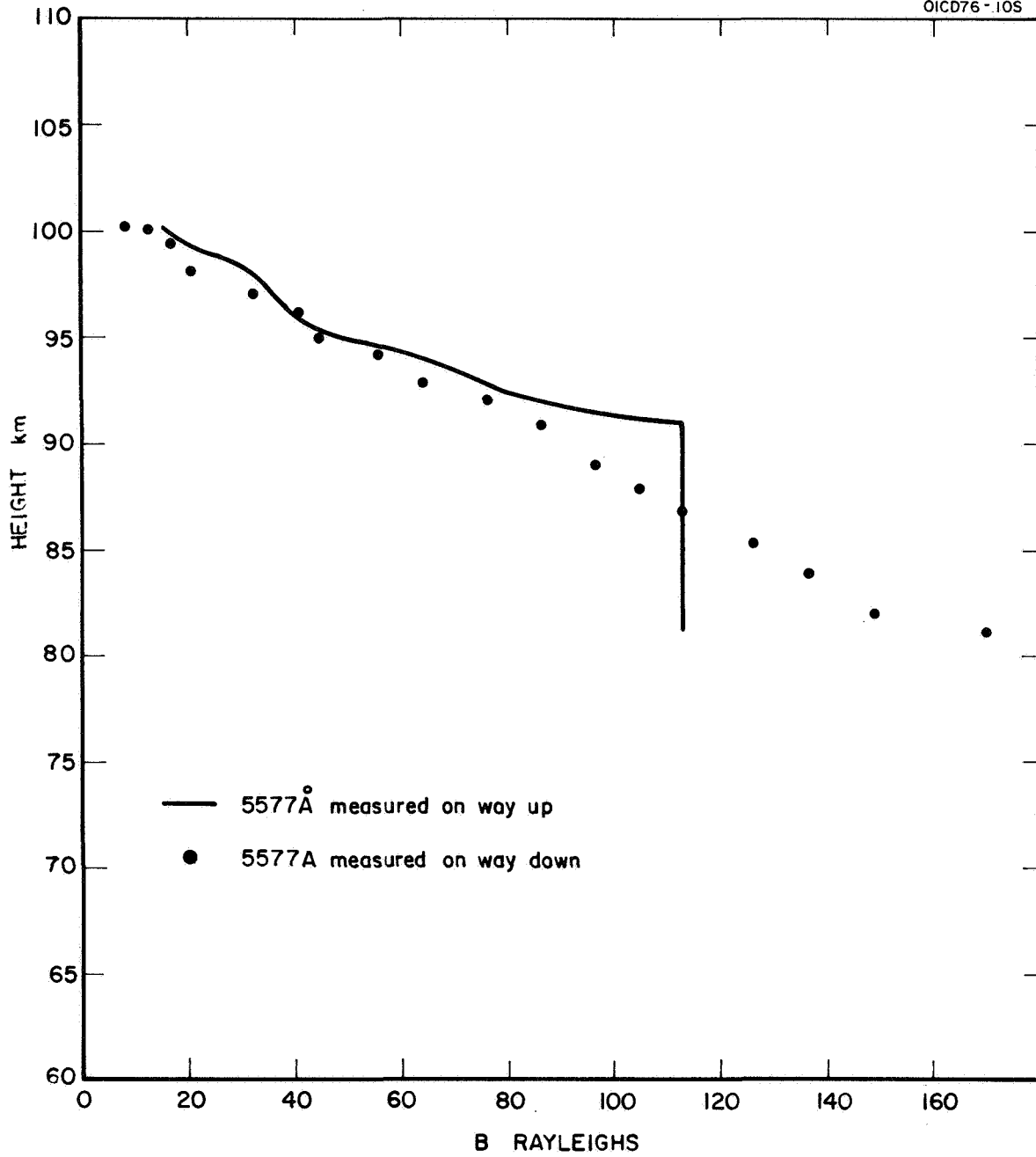
38

Figure 10. Photometer signal.

TABLE 4

A SYNOPSIS OF NIGHTGLOW EMISSION HEIGHTS FROM ROCKETS

Author	Time	Place	Geomag. latitude	Geograph. latitude	(OI)5577Å emission				Filter Å bandwidth
					Peak intensity km	Lower boundary km	Upper boundary km	Half-thickness km	
1. Berg et al.	Nov., 1955	White-Sands New Mexico	41°12′N	32°24′N	92.5	70	105	10	100
2. Koomen et al.	Dec., 1955	White-Sands, New Mexico Data re-examined by Packer	41°12′N	32°24′N	96	80	115	11	20
3. Heppner et al.	July, 1956	White-Sands, New Mexico	41°12′N	32°24′N	97	90	118	7	30
4. Tousey	March, 1957	White-Sands New Mexico Data re-examined by Packer	41°12′N	32°24′N	98	85	107	14	18
5. Cooper et al.	Nov., 1959	White-Sands, New Mexico	41°12′N	41°12′N	96	78	120	14	18
6. Huruhata et al.	Oct., 1961	Michikawa, Japan	28°0′N	39°34′N	98	89	113	7.5	
7. Tarasova	Sept., 1960	Mid-Latitude, U.S.S.R.	N	N	90	82	110	6	
8. O'Brien et al.	July, 1964	Wallops Island, Virginia	48°30′N	37°50′N	94.5	82	105	5.8	61
9. Huruhata et al.	March, 1965	Kagoshima Japan	20°0′N	31°30′N					
10. Gulledge et al.	Oct., 1965	White-Sands, New Mexico	41°12′N	32°24′N	245				
11. Greer & Best*	Oct., 1965	Woomera, S. Australia	41°21′S	30°58′S	94.5	85	110	6.5	64
	Feb., 1968	W.I.			91	91	100	3.5	3
	Average heights (not including*)				95	82	111	9.4	

background emission through a relatively broad filter by comparison with another such filter in a different spectral region and secondly, possible contamination of the optics which disappears later and could be interpreted as an increase in brightness. The photometer used here overcomes both of these difficulties. First, the filter is very narrow and the tilting procedure allows ready comparison between the 5577Å signal and that which obtains only a few angstroms removed. In addition, the entrance optics was protected by the nose cone until approximately 65 km and its operation throughout powered flight was observed to be proper from the response to a pulsed calibration source.

Of course the results of one flight do not justify unlimited conclusions or serious criticism of previous measurements but the similarity of the recorded profile to that expected on a theoretical basis indicates the merits of the oscillating narrow band filter technique and suggests that this and possibly other measurements can be repeated with the improved filters.

C. Spectroscopic Data and Discussion

Through the operation of a Fastie-Ebert ground spectrometer, several twilight trail TEB spectra were obtained at T + 5 and T + 10 minutes. They are given in Figures 11 and 12 respectively while the calibration curve is given in Figure 13. The wavelengths of some of the more prominant features are given in Table 5. The symbol "d" is the displacement for use in the dispersion equation given in Figure 13.

Hoffman et al (Ref. 7) have given a low resolution emission spectrum of a sunlit TEB release (See Figure 14). Their assignment was to the $A\ ^2\Pi - ^2\Pi$ transition of boron oxide but was somewhat confusing because they were unclear as to which oxide of boron was responsible. Subsequently, Millikan (Ref. 8) gave a different assignment — that of the BO_2 boric oxide "fluctuation bands" (see Table 6).

A preliminary and tentative assignment has been made of the four prominent features of the spectrum taken at T + 10 minutes. Such an assignment is difficult because of the overlap of the second and third order and because of the gap in wavelengths between 4754Å and 5826.6Å between the second and third order. In Table 7 are given the four major features designated A, B, C, D whose assignment is discussed below.

A and B are ascribed to second order at 5826.6 and 5848.1Å respectively. They are assigned to the BO_2 X $^2\Pi$ - A $^2\Pi$, 000 - 100 band system. The C peak, ascribed to the third-order spectra, has a wavelength of 4072.2Å. The assignment is to the X 000 $^2\Pi_{0\frac{1}{2}}$ - B 000 $^2\Sigma^+$ transition. The D peak ascribed to the third order has a wavelength of 4467.0Å. It is assigned to the X $^2\Pi_g$ - A $^2\Pi_u$, 000 - 100 band system. All of the assignments are based
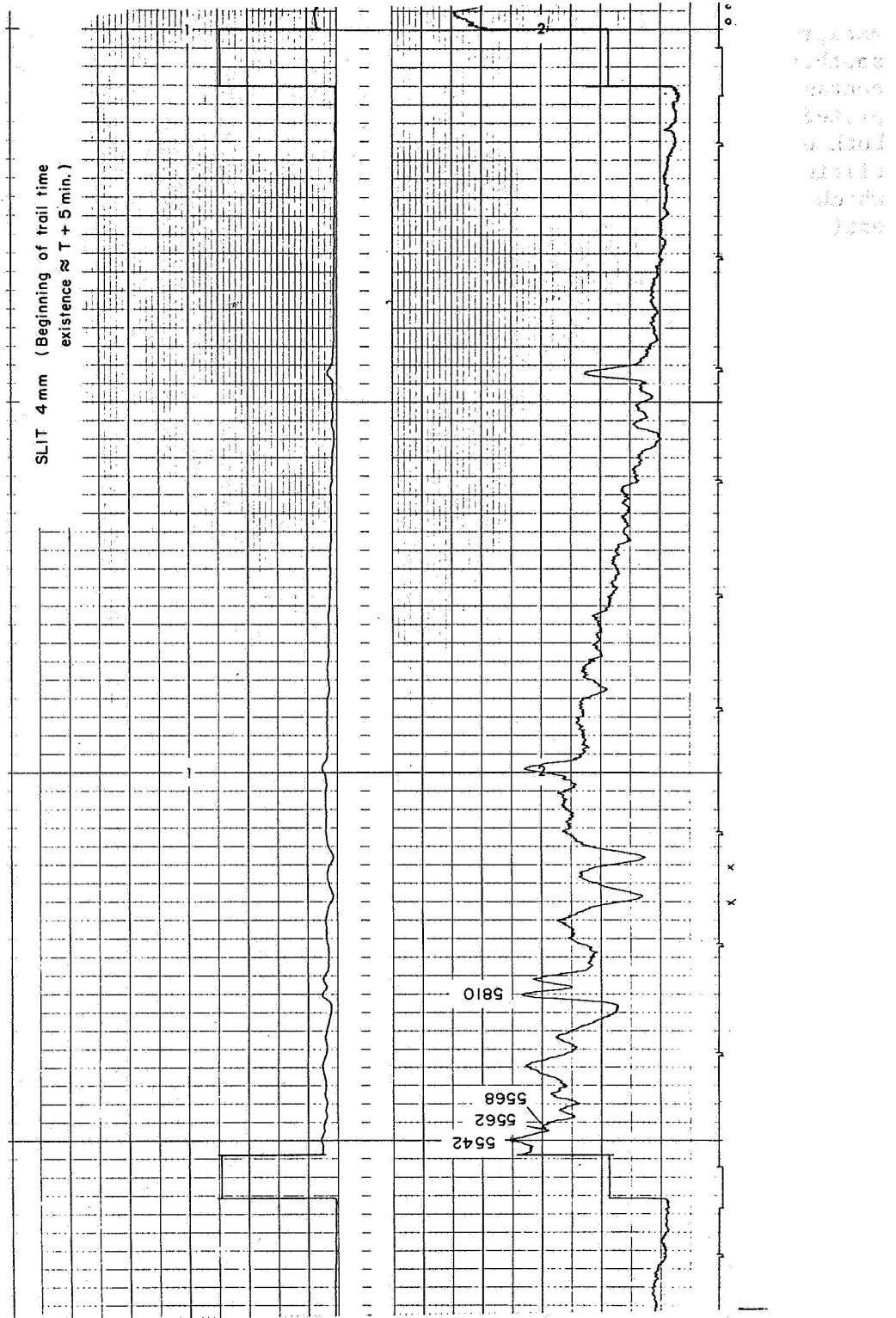
Figure 11. Twilight TEB spectrum at T + 5 minutes.

42
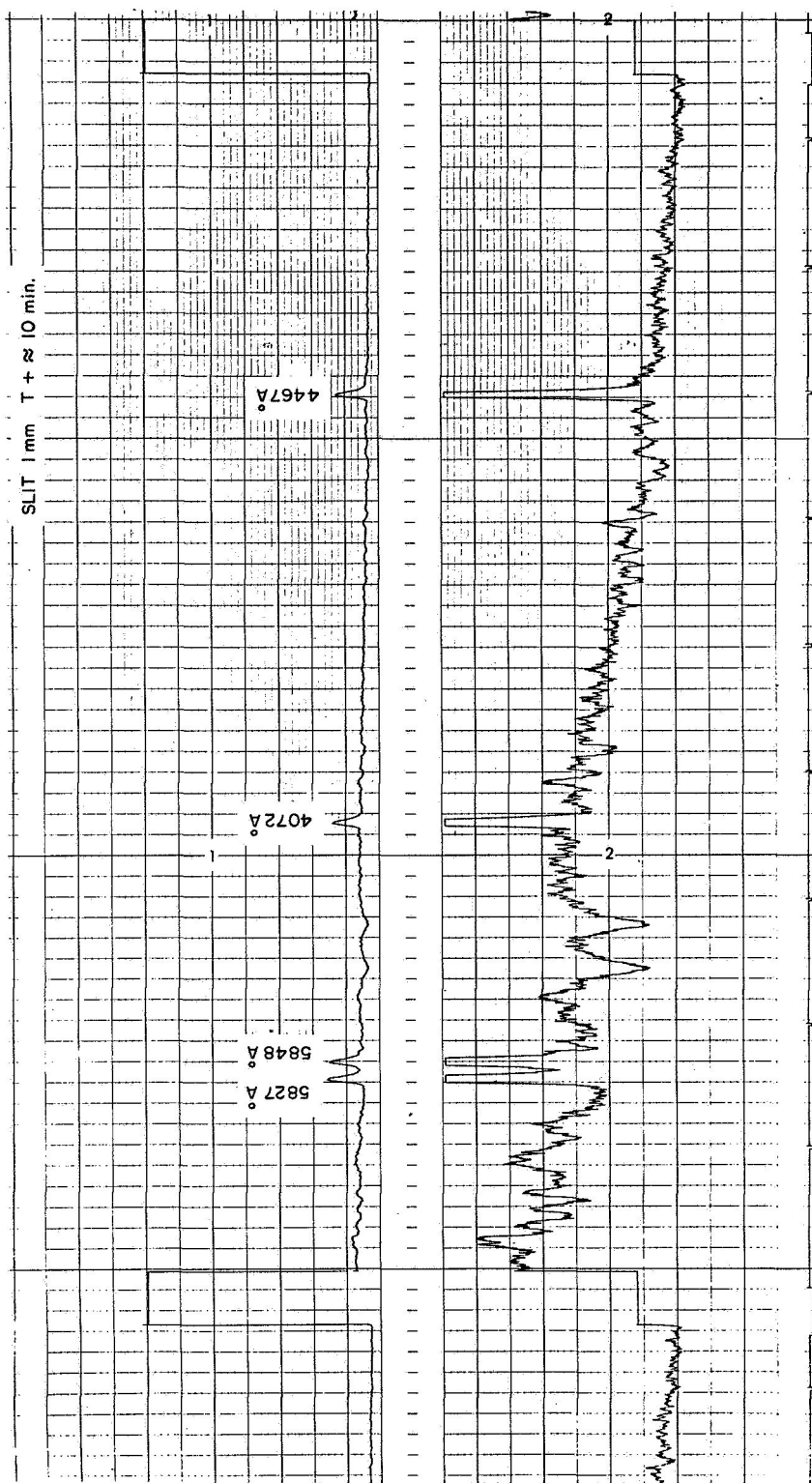
Figure 12.   Twilight TEB spectra at T + 10 minutes.

DISPERSION ASSUMED: $\lambda = a d^2 + bd + c$ $a = 3.6081 \times 10^{-3}$
d = displacement $b = 10.348$ Å/mm
$c = 11057$ Å

4 x 3341.5

3 x 4358

3 x 4347
3 x 4339

4 x 3132
4 x 3126

1

2

3 x 4078

3 x 4047

4 x 3024

4 x 2967.3

2 x 5790
2 x 5770

Hg lamp Calibration

Assignments

2 x 5528.5

d = 0

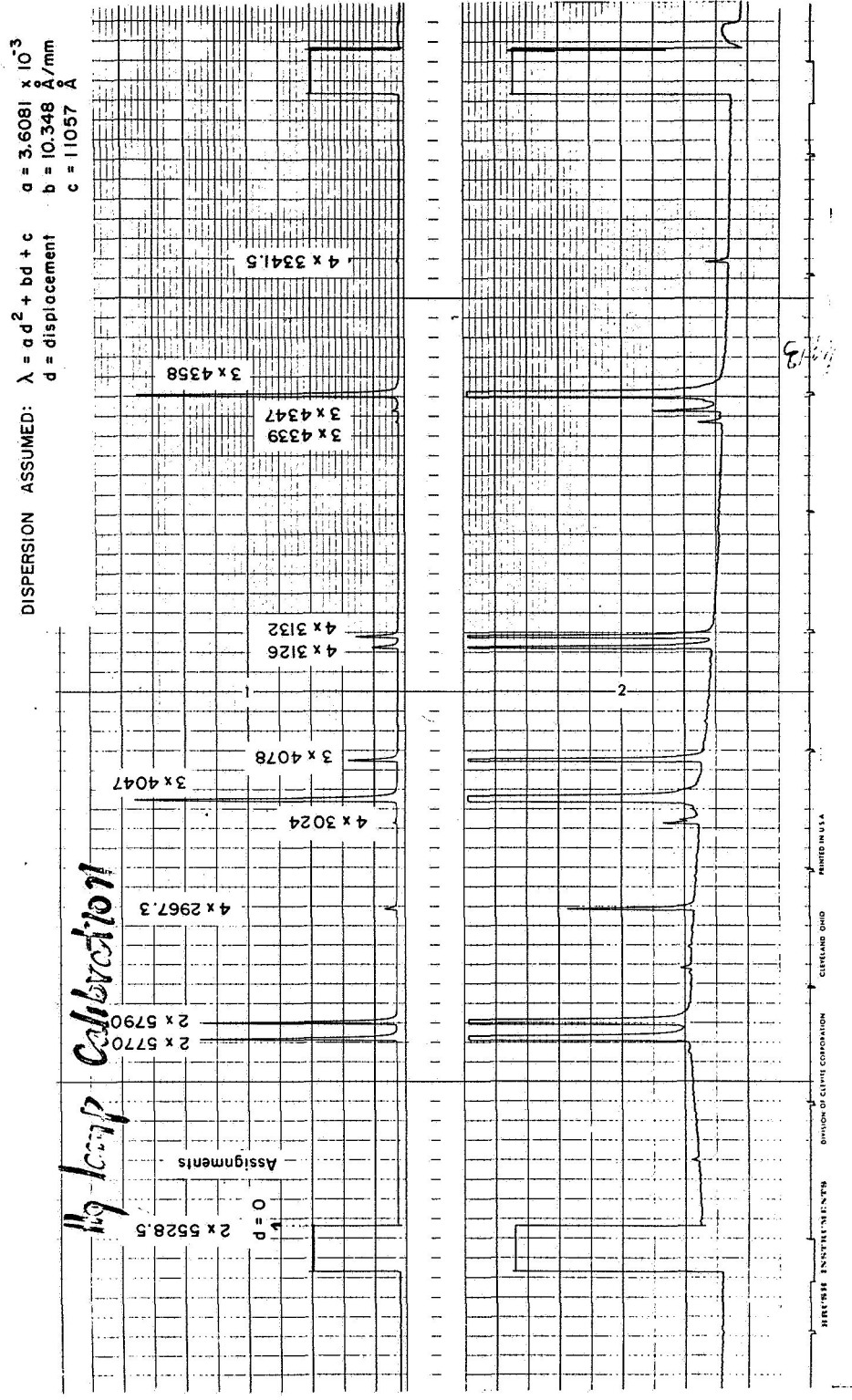PRINTED IN U.S.A.   CLEVELAND OHIO   DIVISION OF CLEVITE CORPORATION   BRUSH INSTRUMENTS

Figure 13. Calibration spectra of spectrometer.

TABLE 5

SOME PROMINENT FEATURE OF THE TEB
TWILIGHT EMISSION SPECTRA

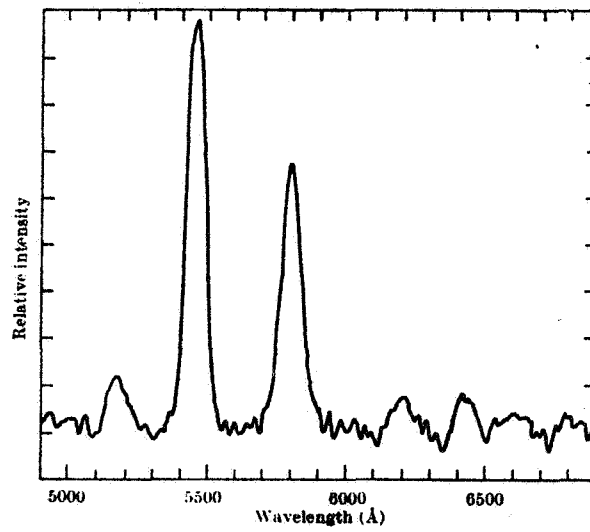| d(mm)	λ Second Order	λ Third Order
(mm)	(Å)	(Å)
2.4	5542	3694
6.5	5562	3708
7.6	5568	3711
11.0	5585	3724
15.0	5606	3737
18.7	5626	3751
26.0	5662	3775
27.5	5670	3780
31.0	5687	3792
34.0	5702	3802
35.5	5710	3807
37.0	5718	3812
38.0	5723	3815
55.5	5810	3874
56.2	5813	3876
58.0	5823	3882
61.5	5840	3893
66.0	5862	3908
73.0	5897	3931
83.5	5948	3965
126.0	6152	4101
180.5 ± 0.2 mm	6404 ± 1Å	4269 ± 1Å

Figure 14. Spectrum obtained from the sunlit
release of triethyl boron at height
between 90 km and 178 km. (Ref. 7)

TABLE 6

(Taken from Ref. 8)

EMISSION MAXIMA FROM UPPER ATMOSPHERE RELEASE	ABSORPTION MAXIMA FOR BO_2 IN FLAMES
6,420	-----
6,200	6,200
5,795	5,790
5,465	5,470
5,170	5,180

TABLE 7

MAJOR FEATURES OF TWILIGHT SPECTRUM
OF TRIETHYL BORON RELEASE

Code of Prominent Feature	d(mm)	Wavelength ($\overset{\circ}{A}$)		
		1st Order	2nd Order	3rd Order
A	56.5	11653.3	5826.6	3884.4
B	60.5	11696.2	5848.1	3898.7
C	108.0	12216.7	6108.3	4072.2
D	211.0	13401.0	6700.5	4467.0

The above features calculated from dispersion formula

$$\lambda = ad^2 + bd + c \quad (\overset{\circ}{A})$$

where $a = 3.608 \times 10^{-3}$, $b = 10.348$, $c = 11057$.

on the analysis given in Mavrodineau (Ref. 9) and particularly the high resolution analysis of Johns (Ref. 10). They are favorable fluorescent transitions beginning at the heavily populated $0\overset{o}{0}0$ vibration level of the ground state. The C line at $4072.2\overset{o}{A}$ represents a transition not observed previously in the Sandia twilight observation of TEB due to the fact that the spectrometer they used did not extend below $4900\overset{o}{A}$.

D. Concluding Remarks

The following remarks are of a preliminary nature pending the full analysis of the data obtained on the two rocket flights:

(1) The payload appears to be sound and stable. The nose release works well and is an independent self-contained system. The rocket-borne photometer also appears good although some changes are needed. It also operates independently and thus may be used with other experiments.

(2) The observed profile of the $5577\overset{o}{A}$ emission has a sharper lower boundary, a more rapid decrease with height and thus a much smaller half width than previous similar altitude profile measurements. The differences are so great that the new measurements require verification even though they more closely resemble the expected profile. If the new profile is proven to be accurate, measurements to determine seasonal and latitudinal effects may be desirable. Profiles of other airglow lines may also be obtained.

(3) It must be concluded on the basis of the evidence available that TEB does not chemiluminesce in the upper atmosphere contrary to laboratory evidence. The full reasons for this are not determined at the present time.

(4) The TEB trail appears as bright as TMA at twilight. The question of temperature determination must wait until such a time as the fine structure has been resolved with a view toward the possible separation of the BO and BO_2 emissions.

(5) A new BO_2 band, not observed in the previous twilight spectrum has been observed. The band is at $4072.2\overset{o}{A}$ and assigned to the $X\,^2\,\Pi_{o\frac{1}{2}}$ - $B\,^2\Sigma^+$, $0\overset{o}{0}0$ - $0\overset{o}{0}0$ transition unlike the other transitions assigned to the X-A states.

REFERENCES

1. Rosenberg, N.W., D. Golomb and E.F. Allen, Jr., J. Geophys. Res., <u>68</u>, 5895 (1963).

2. Rosenberg, N.W., D. Golomb and E. F. Allen, Jr., J. Geophys. Res., <u>69</u>, 1451 (1964).

3. Pressman, J., A. Sharma, J.P. Padur, H. Brown, and C. Rosen, "Upper Atmosphere Chemical Release Study," GCA Final Report No. GCA 65-23-N (1965).

4. Pearse, R.W.B. and A.G. Gaydon, <u>The Identification of the Molecular Spectra</u>, John Wiley and Sons, Inc., N.Y. (1963).

5. Stair, Schnider and Jackson, "A New Standard of Spectral Irradiance," Applied Optics, <u>2</u>, 1151 (1963).

6. Greer, R.G.H. and Best, G.T., "A Rocket-Borne Photometric Investigation of the Oxygen Lines at 5577$\overset{\circ}{A}$ and 6300$\overset{\circ}{A}$, the Sodium D-Line and the Continuum at 5300$\overset{\circ}{A}$ in the Night Airglow, PASS, <u>15</u>, 12, Dec. 1967.

7. Hoffman, J.M., Nature, <u>215</u>, 115-8 (1967).

8. Millikan, R.C., Nature, <u>216</u>,(Nov. 11, 1967)

9. Mavrodineau, R. and Borteux, H., <u>Flame Spectroscopy</u>, John Wiley and Sons, Inc., N.Y.

10. Johns, J.W.C., Canadian J. Phys., <u>39</u>, 1738 (1961).